https://ntrs.nasa.gov/search.jsp?R=19670030622 2020-03-16T16:48:39+00:00Z

report

WYLE LABORATORIES - RESEARCH STAFF
REPORT WR 65-21

AIR SHOCK PARAMETERS AND DESIGN CRITERIA FOR ROCKET EXPLOSIONS

GPO PRICE $ _____

CFSTI PRICE(S) $ _____

Hard copy (HC) 3.00

Microfiche (MF) .65

ff 653 July 65

WYLE LABORATORIES
TESTING DIVISION, HUNTSVILLE FACILITY

FACILITY FORM 602

N67-39951 (ACCESSION NUMBER) (THRU)

96 (PAGES) 1 (CODE)

CR#89622 (NASA CR OR TMX OR AD NUMBER) 31 (CATEGORY)

research

R-147193

WYLE LABORATORIES - RESEARCH STAFF
REPORT WR 65-21

AIR SHOCK PARAMETERS AND DESIGN CRITERIA FOR ROCKET EXPLOSIONS

By

F. V. Bracco

This report is submitted as partial completion of work under Contract NAS 8-11217

Prepared by F. V. Bracco
F. V. Bracco

Approved by K. McK. Eldred
K. McK. Eldred

Approved by L. C. Sutherland
L. C. Sutherland

Date September 1965

ABSTRACT

This report contains specific design charts and recommendations for the calculations of rocket explosion air blast parameters of interest in structural load calculations. Parameters, based on far-field-TNT-equivalencies are defined for the far-, medium-, and close-field of rocket explosions. For the far- and medium-field, the far-field-TNT-equivalencies are believed to give sufficient accuracy while for the close-field they are believed to give conservative results. In the present report, examples are given for the far- and medium-field blast parameters. The blast parameters charts for the medium-field can also be used for the close-field if desired; however, it is the author's intent to present more realistic values for the close-field air blast parameters in a later report. In the appendices more detailed consideration is given to several pertinent aspects of the rocket explosion problem. Statistical analysis of propellant explosion data (to determine TNT equivalencies for large rockets), initial air shock velocities, rate of energy release, and far-field focusing effects are recognized as critical areas for which further studies are suggested.

TABLE OF CONTENTS

TABLE OF CONTENTS (Continued)

LIST OF TABLES

LIST OF FIGURES

LIST OF FIGURES (Continued)

LIST OF FIGURES (Continued)

LIST OF SYMBOLS

c	=	speed of sound
d	=	ground zero blast distance (unless otherwise specified)
E	=	total energy
h	=	blast altitude
I	=	impulse
p	=	pressure
q	=	dynamic pressure
R	=	shock radius
t	=	time; duration
u	=	particle velocity
U	=	shock velocity
WT	=	weight
Z	=	reduced distance = $R/(WT)^{1/3}$

Greek Symbols

ρ	=	density
λ	=	dimensionless distance = $R/(E/\rho_0)^{1/3}$

Superscripts

0	=	ground level
+	=	positive phase

Subscripts

0	=	undisturbed conditions
r	=	reference value
s	=	shock front value
p	=	overpressure parameter
q	=	dynamic pressure parameter

1.0 INTRODUCTION

The problem of possible rocket explosions is of considerable interest to the aerospace industry and government agencies. This interest is due not only to safety considerations but to economic factors as well. Usually the positioning of storage, testing, and launching areas is based on possible explosion hazards. The present report is part of a series of reports, prepared under NASA Contract NAS8-11217, in which the rocket explosion problem has been studied primarily from a damage viewpoint. In Wyle Laboratories Report WR 64-11, the extensive theory of blast generation was investigated in detail. In the present report, design charts for air shock parameters for overpressures smaller than 14.7 psi are given. In subsequent reports, air shock parameters for overpressures greater than 14.7 psi will be defined more accurately and air shock loads on structures and structural response to blast will be covered. It is believed that one of the main contributions of this series of reports is the clear recognition that the overpressure close to a rocket explosion site is considerably smaller than what is presently estimated by extrapolating far-field measurements. For these later reports, calculations will actually be performed, the main assumption being that the initial air shock velocity is equal to the detonation velocity of the explosive. This assumption, while in contrast with the present air shock origin theories, is supported by experimental results and can be supported by an improved air shock origin theory. Although it is recognized that the total energy released is still the main unknown which can be determined only by large scale experiments, it is also believed that a proper combination of experimental data on energy released and our close-field theory would lead to considerable saving when close-field structures, like launching facilities and bunkers, are designed. The remainder of this introduction consists of a description of a rocket explosion and of the air shock which follows. This description is elementary while introducing the main physical nature of a rocket explosion. If only charts and examples of applications for overpressure less than 14.7 psi are of interest, sections 2 and 4 can be used directly.

1.1 The Origin of the Air Shock

A rocket is a volume within which energy is stored in the form of propellants. In order for this energy to be released, proper conditions, characteristic of each propellant, must be reached. If these conditions are reached under an uncontrolled situation, an uncontrolled chemical reaction occurs. This chemical reaction can either be a deflagration or a detonation (Appendix A). A deflagration creates a pressure wave in air which is far less important, from a structural design viewpoint, than the wave produced by a detonation. Consider a mixture of liquid propellants resulting from a tank rupture and assume that a detonation starts at a point in the mixture. Then the detonation propagates through the mixture at high speed until the interface between the propellant mixture and air is reached. At this point a volume of high energy gases is present, where the propellant mixture existed previously. The gases, surrounded by an atmosphere at lower pressure, expand outward, thus generating a wave in the atmosphere itself. This wave is called a shock wave, because the air properties change suddenly

at its front. The front of the shock is a sphere with the center at the explosion site. The shock front moves outward at supersonic speed and it is followed by a high velocity hot wind. On the shock front, the pressure, density, and temperature of the air rise almost instantaneously, to decay rapidly afterward. Eventually, the pressure and density will decay to values lower than their original ambient values and the wind will reverse its direction. Finally, the pressure and temperature will return to ambient levels and the blast wind will cease. The variations of pressure, density, temperature, and particle velocity with time and distance are qualitatively illustrated in Figure 1.

1.2 Air-Shock Ground Interactions

So far an explosion in an unbounded space has been described. This is the case of a rocket exploding at a high altitude. If the explosion occurs on the ground surface, the air blast parameters qualitatively will change with time and space approximately as for an unbounded explosion releasing twice as much energy.

When the explosion occurs during the initial part of the flight near the ground, the shock pattern is slightly more complicated. In this case the shock is reflected when it reaches the ground and the incident and reflected shocks originate a third shock called the "Mach Stem" which is normal to the ground at the ground level. The blast parameters as experienced by an observer standing on the ground may now be different from those previously described. Sketch A of Figure 2 illustrates the reflection process. Sketch B illustrates a particular aspect of the reflection process; the generation of the "Mach Stem". It was stated above that a strong wind follows the shock front. A similar wind follows also the reflected shock. This wind has to be parallel to the ground. This particular direction of the wind is not always compatible with a two - shock configuration and thus, a third shock is required. The third shock is the "Mach Stem", and is stronger than both the incident and reflected shocks. Before the formation of the "Mach Stem", in what is called the "Regular Reflection Region", an observer, somewhat above the ground level, would actually experience two shocks. After the formation of the "Mach Stem" an observer would experience one or two shocks according to whether he is located below or above the triple point surface (Sketch C, Figure 2).

1.3 Elements Determining the Air Shock Parameters

The explosion elements, which influence the air shock parameters most, are: explosion energy, explosive mass to energy ratio, rate of energy release, initial air shock velocity, and weather conditions.

It is evident that the explosion energy is a major element. Very roughly multiplying the energy by 9, the peak overpressure at a given distance would be 3 times larger, or the distance at which the same pressure is measured would be 3 times as large and the durations would be 3 times as long. Unfortunately, very few theoretical observations of limited usefulness can be made about the amount of energy possibly released

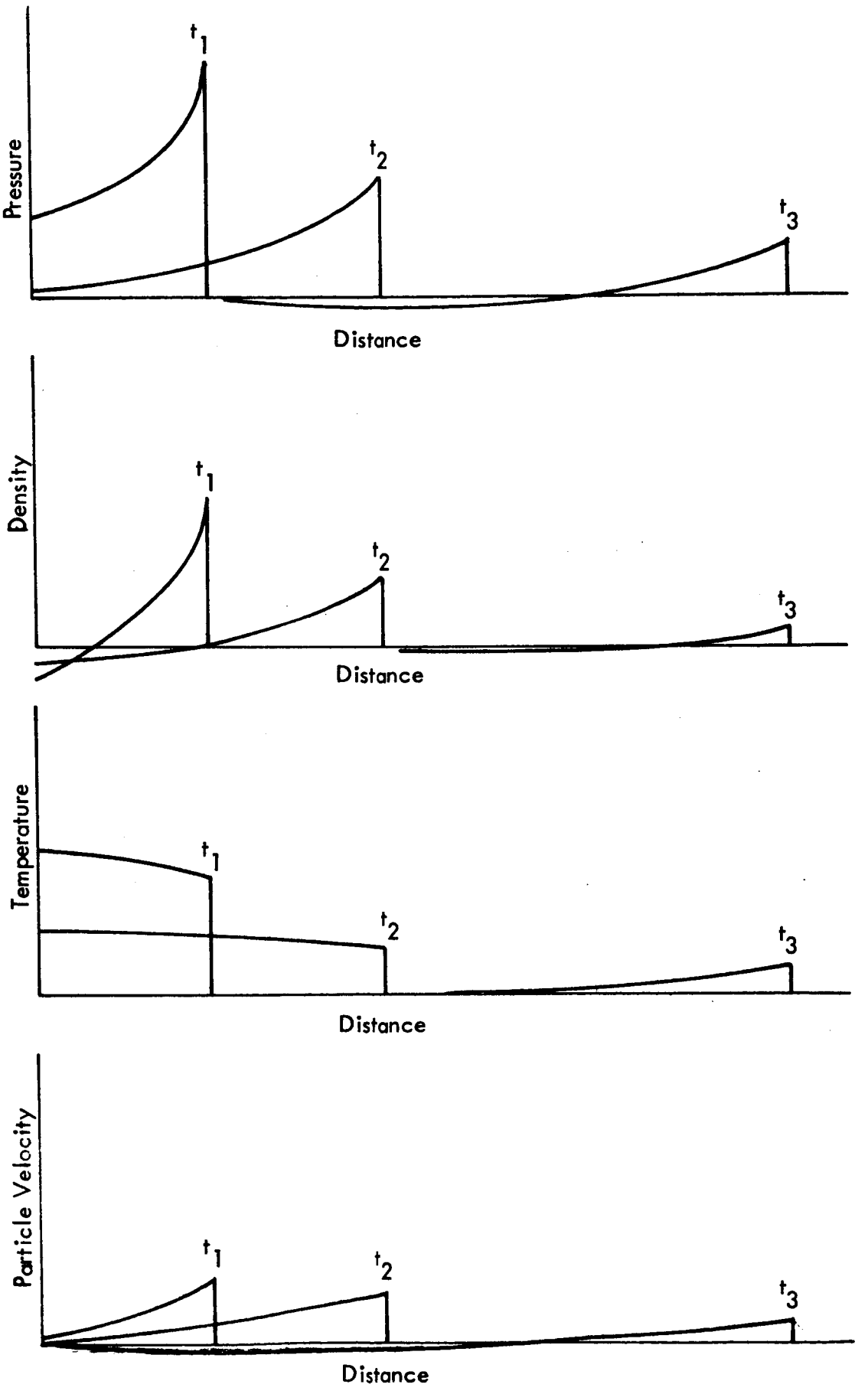

Figure 1. Qualitative Variations of Air Blast Parameters with Distance and Time

Sketch A

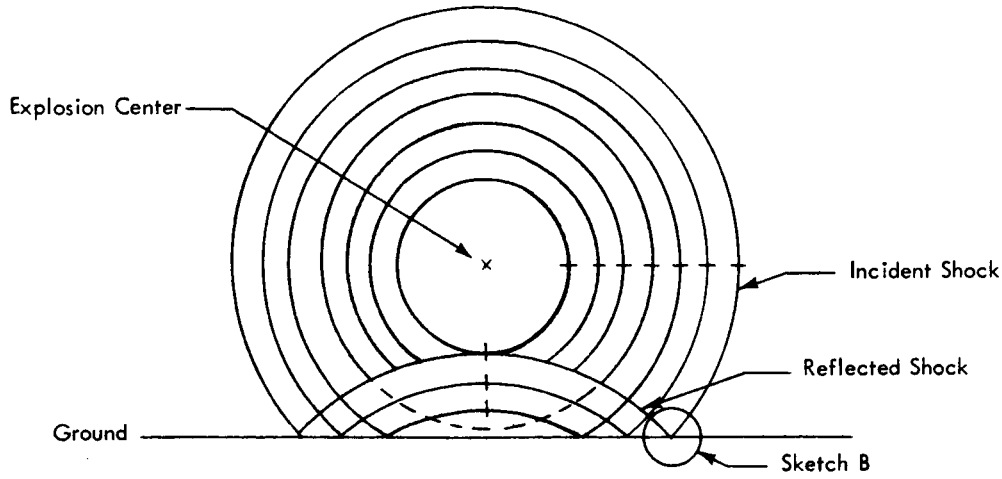

Sketch B

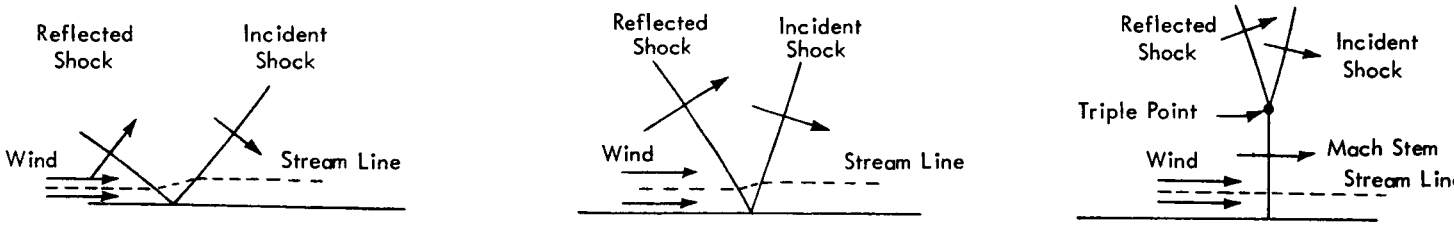

Sketch C

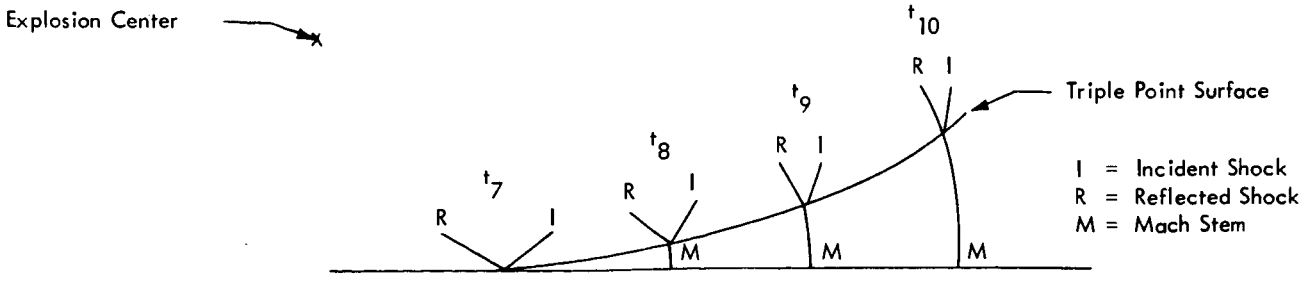

Figure 2. Ground Reflection of a Spherical Blast Wave and Mach Stem Formation

in a rocket explosion. Although attempts to predict the energy release have been made, (Reference 6), it is generally accepted that realistic rules can be defined only from the statistical analysis of experimental data.

On the other hand, explosive mass to energy ratio, rate of energy release and initial air shock velocity influence the air blast parameters up to a certain distance from the explosion site. This distance determines a region which is called the "close-field", and for large rocket explosions (5×10^6 lb. far-field-TNT-energy-equivalent) this region is actually rather large and extends out to distances of the order of one thousand feet or more, with peak overpressures down to about 1 At. Within the close-field, where launch structures are actually located,the peak overpressure for a rocket explosion could be about 4 times lower than the peak overpressure for a TNT explosion with the same energy release. Thus, from a practical viewpoint, proper knowledge of the close-field air shock parameters is comparable in importance to proper knowledge of the total energy released.

Finally, for very large distances, weather effects become as important as the total energy. Communities located at a distance of 20 miles would suffer no damage from a rocket explosion of 5×10^6 lb. TNT energy equivalent for a uniform atmosphere. The peak overpressure would be .04 psi and window breakage would normally not be expected. But under extreme atmospheric focusing conditions, the local peak overpressure can be multiplied by a factor of 5, thus, reaching an overpressure which would normally be expected by an explosion roughly 5 times larger and window breakage would very likely occur.

The above considerations show that in the close-field the effects of the nature of the explosive, and in the far field, the effect of focusing can be as important as a factor of 5 in the energy estimate as far as practical problems are concerned. Some further considerations on the definition of the close-field will follow, while the problem of focusing will be considered only in a later report.

1.4 The Close-Field: Explosive Mass to Energy Ratio; Rate of Energy Release; Initial Air Shock Velocity

The close-field is the region within which the air blast parameters are functions of explosive mass to energy ratio, rate of energy release, initial air shock velocity,and probably other physical and chemical properties of the explosive, besides being functions of the total energy released. Practically, when the above definition is applied, the close-field radius can be estimated for each explosive and explosion energy. The peak overpressure at the outer radius of the close field can also be determined for each explosive, independently of the explosion energy. In this section these peak overpressures and close-field radii for particular explosion energies will be estimated for LH_2 - LO_2 and RP-1-LO_2 rocket explosions. Also the initial values of the air shock peak overpressures will be estimated. When initial and final peak overpressures and initial and final radii are known, the close field can be considered determined.

In the remainder of the present section first a principle to take into account the influence of the mass to energy ratio is stated; second, this principle is applied to TNT, LH_2 - LO_2 and RP-1-LO_2 explosions to find the peak overpressures at the limits of the close-field; third, an energy is chosen and close-field radii and initial peak overpressures are estimated and finally the above results combined and ranges of the peak overpressures given for this close-field.

In Taylor's similarity solution for strong shocks, (Reference 1), the mass of the explosive with respect to the mass of air within the shock is neglected. Taylor pointed out that his results should be independent of the nature of the explosive when the mass of air within the shock is considerably larger than the initial mass of the explosive. Prior to this, Taylor and then Bethe, (Reference 2), noticed that it takes a considerable time for the energy to transfer from a concentrated explosive charge to the surrounding air, owing to the great difference in density between these two media. Thus, during all this period, the pressure in the air shock is less than it would be for a point source explosion liberating the same energy. The same argument can be repeated in comparing explosions of concentrated charges like TNT with explosions of propellants because the rate of energy release in propellant explosions is much smaller than the corresponding rate in TNT explosions. Finally, Brode (Reference 3 - 1955), found that solutions for a point source explosion and for two hot isothermal spheres with starting overpressures of 2002 and 121 At., respectively,and equal densities inside and out, become equal when the air engulfed by the shock front is equal or larger than 10 times the initial mass of the hot gases. From all the above considerations it follows that the definition of the far field has to respect the "10 times the initial mass of explosive" criterion since, by definition, the far-field is the region where the blast parameters are independent of the type of explosion and depend only on the total energy released.

When the "10 times the initial mass" concept is applied to a TNT surface explosion, the outer radius of the close-field or inner radius of the far-field is found as follows:

$$10 \cdot WT = \frac{2}{3} \cdot \pi \cdot (C.F.R)^3_{TNT} \; \rho_0$$

$$\therefore \; (C.F.R.)_{TNT} = (15 \cdot WT/\pi \cdot \rho_0))^{1/3}$$

where $(C.F.R.)_{TNT}$ stands for "close-field radius for TNT". The scaled distance, $\lambda_{surface}$, can now de determined for $(C.F.R.)_{TNT}$ using the definition:

$$\lambda_{surface} = \frac{R}{(E/P_0)^{1/3}} = .112 \cdot \frac{R}{(WT)^{1/3}}$$

and setting

$$R = (C.F.R.)_{TNT}:$$

$$\lambda_{surface} = 0.112 \cdot (15 \cdot WT/(\pi \cdot \rho_0))^{1/3}/(WT)^{1/3} = 0.112 \cdot (15/(\pi \cdot \rho_0))^{1/3} = 0.445$$

Entering Figure 3 with this value of $\lambda_{surface}$ and reading on the "TNT calculated and measured curve", the peak overpressure at which the TNT close-field ends and the far-field begins, is found to be 4.46 At.

The "10 times the initial mass" concept can now be extended to $LH_2 - LO_2$ and RP-1-LO_2 explosions. Usually the mixture ratio for $LH_2 - LO_2$ is 1:5, and for RP-1-LO_2 is 1:2.25. The Stoichiometric mixture ratios are 1:8 and 1:3.5 (approximately), respectively. The stoichiometric heats of combustion are 51,500 and 18,500 Btu/lb, respectively. Since the usual mixture ratios are not stiochiometric, 40,000 and 16,000 Btu/lb, respectively, are assumed to be the maximum heats of combustion. Thus, 6 lb of $LH_2 - LO_2$ give 40,000 Btu and 3.25 lb of RP-1-LO_2 give 16,000 Btu. The specifications recommended in Reference 4, are that 60 percent and 10 percent of the weight of the above two propellant combinations shall be the weight of the TNT equivalent explosive energy (see Table I). Since 1 lb of TNT releases 1,940 Btu, 6 lb of $LH_2 - LO_2$ yield (0.6 x 6) x 1,940 = 7,000 Btu when they explode. Similarly 3.25 lb of RP-1-LO_2 yield (0.1 x 3.25) x 1,940 = 630 Btu. Since 6 lb of LH_2-LO_2 release 7,000 Btu instead of 40,000 Btu, either only part of the 6 lb actually explode and the remaining will burn, or all 6 lb actually explode with low efficiency. Specifically, either only 6 x 7,000 Btu/40,000 Btu = 1.05 lb of propellant explode with 100 percent chemical efficiency and 4.95 lb will burn or all the 6 lb of propellant explode with a chemical efficiency of 7,000 Btu/40,000 Btu = 17.5 percent, or anything between 1.05 and 6 lb actually explode with a chemical efficiency varying between 100 and 17.5 percent. Repeating the same reasoning for RP-1-LO_2, anything between .128lb and 3.25 lb actually explode with a chemical efficiency varying between 100 percent and 3.94 percent. The extremes of chemical efficiencies for both $LH_2 - LO_2$ and RP-1-LO_2 have to be excluded. Moreover, the percent of propellant which does not take active part in the explosion, still shares the energy released thus reducing the actual energy conveyed to the air shock at the beginning of its propagation. Thus, 5 lb for $LH_2 - LO_2$ and 3 lb for RP-1-LO_2 appear to be reasonable choices for the weights of propellant taking active part in the explosions. The factor of 5 for $LH_2 - LO_2$ and of 3 for RP-1-LO_2 can be used to define the peak overpressures at the outer limits of their respective close-fields. Thus, for

$$LH_2 - LO_2: \quad \lambda_{surface} = (5)^{1/3} \cdot (0.445) = 0.76$$

and

$$RP\text{-}1\text{-}LO_2: \quad \lambda_{surface} = (3)^{1/3} \cdot (0.445) = 0.642$$

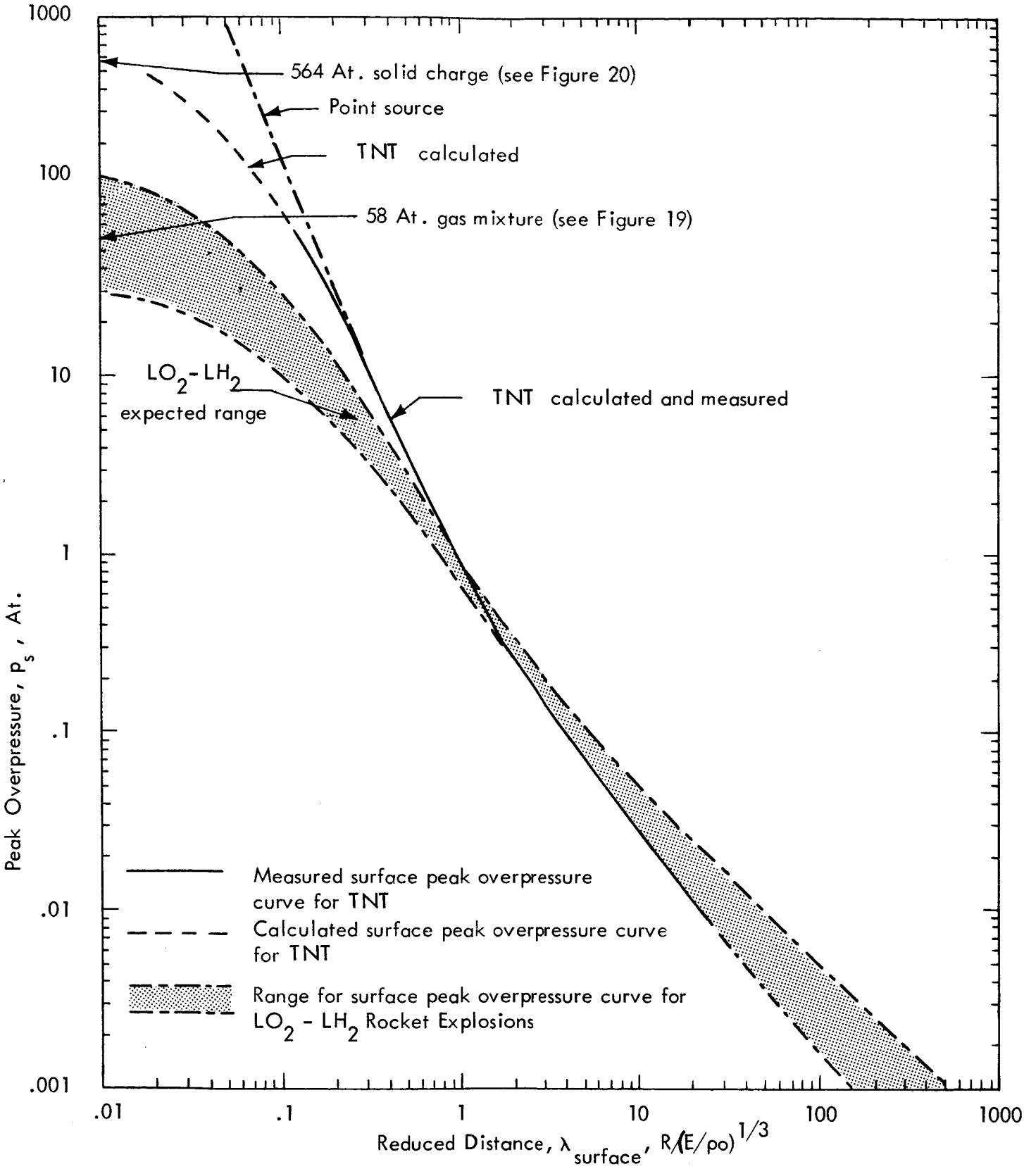

Figure 3. Range within which Surface Peak Overpressure Curve for Explosions of LO_2 - LH_2 Rockets is Expected to Fall, Compared with Measured Surface Peak Overpressure Curve for TNT Explosions of Equal Total Energy

from which the peak overpressures are found to be 1.5 At. for $LH_2 - LO_2$ and 2.0 At. for $RP\text{-}1\text{-}LO_2$. The above does not take into account the rate at which energy is released. The importance of this is illustrated by the limit case of normal combustion in which the energy is released so slowly that it can be distributed into the surrounding air by convection, conduction, and radiation. In this case, no shock would be generated. A few notes on the rate at which energy is released are found in Appendix A. Here it will suffice to say that since the rate of energy release for propellants is actually small, the above suggested factors of 5 for $LH_2 - LO_2$ and of 3 for $RP\text{-}1\text{-}LO_2$ have to be considered as minimum factors, and the relative peak overpressures of 1.5 At. and 2.0 At. as maximum values of overpressures for which TNT charts can be used in predicting air blast parameters from explosions of the above propellants.

In Section 3, possible future chemical rocket configurations are considered and the energies that they might be able to release in the event of an explosion calculated using the Department of Defense safety specifications for TNT equivalents issued in 1964, (Reference 4). The maximum far-field TNT equivalent computed is 12.83×10^6 lb. However, it must be pointed out that the above specifications are conservative, where large rockets are concerned, because they are based on experiments with small charges in which case a high percentage of the propellants are actually involved in the explosion. Thus, instead of 12.83×10^6 lb TNT we arbitrarily estimate that 5×10^6 lb far-field TNT can be used as an approximate upper bound of actual explosive energy for future chemical rockets. When the "10 times the initial mass" concept is applied to a 5×10^6 lb TNT surface explosion, it is found that the close-field maximum radius $(C.F.R.)_{TNT}$ is given by:

$$10 \cdot (5 \cdot 10^6) = \frac{2}{3} \cdot \pi \, (C.F.R.)^3_{TNT} \quad \rho_0$$

$$\therefore \; (C.F.R.)_{TNT} = 679 \text{ ft.}$$

When the same concept is applied to $LH_2 - LO_2$ and $RP\text{-}1\text{-}LO_2$ explosions together with their mass factors (5 for $LH_2 - LO_2$ and 3 for $RP\text{-}1\text{-}LO_2$), their maximum close-field radii are found to be:

$$(C.F.R.)_{LH_2 - LO_2} = (5)^{1/3} \times (C.F.R.)_{TNT} = 1160 \text{ ft.}$$

$$(C.F.R.)_{RP\text{-}1\text{-}LO_2} = (3)^{1/3} \times (C.F.R.)_{TNT} = 995 \text{ ft.}$$

for 5×10^6 far-field TNT equivalent explosions.

In Appendix B a criterion to calculate the initial peak overpressure is presented and supported with experimental results. The criterion is that the initial air shock velocity is assumed to be the detonation velocity of the explosive. Unfortunately, a rather

extensive search revealed only one set of experimental data for the detonation of a liquid hydrogen/liquid oxygen mixture (2.3 km/sec.), and for the detonation velocity of RP-1/liquid oxygen (2.2 km/sec.) (Reference 5). According to the proposed assumption, using the above detonation velocities, the initial air shock pressure would be 54 and 50 At., respectively. Available data on detonation velocities of gaseous mixtures support the hypothesis of liquid mixtures detonation velocities in the 2 to 3 km/sec. range.

Knowing the initial air shock pressure and the range within which this pressure will be smaller than that from a TNT explosion of equal energy; that is, knowing the peak overpressures at which the close-fields end , an estimate can be made of the probable range of surface peak overpressures from liquid propellant rocket explosions. This range is given in Figure 3. As previously stated, present plans are that accurate calculations for this range will be performed and presented in a later report. Finally, Figure 4 gives the distances for which the far-field TNT equivalencies lead to considerable error for the case of a 5×10^6 lb far-field TNT equivalent rocket explosion. Notice that the values of Figure 4 are for very large rockets. Figure 4 is a graphic representation of the following self explanatory Table whose values are read from Figure 3:

Distance R	Scaling Factor	Peak Overpressure		Reduced Distance	Mass * of Air	Range of Estimated Peak Overpressure
ft.	$Z_1 = \frac{R}{\sqrt[3]{WT}}$	psi	At.	$\lambda = .112 Z_1$	lb/10^6	At.
300	1.75	400	27.20	0.195	4.3	5.6 - 13
600	3.51	90	6.12	0.390	34.5	2.5 - 4.0
900	5.26	36	2.45	0.585	116.5	1.5 - 2.0
1200	7.01	19	1.29	0.780	277.0	0.90 - 1.29
1500	8.77	12.5	0.85	0.975	560.0	~ 0.85
1800	10.53	9.0	0.61	1.170	930.0	~ 0.61
2100	12.29	6.8	0.46	1.305	1490.0	~ 0.46
2400	14.00	5.3	0.36	1.555	2210.0	~ 0.36
2700	15.75	4.4	0.35	1.750	3130.0	~ 0.30

*Mass of Air $= \frac{1}{2}\left(\frac{4}{3}\pi R^3\right)\rho_0$ where $\rho_0 = .07877$ lb/cu.ft.

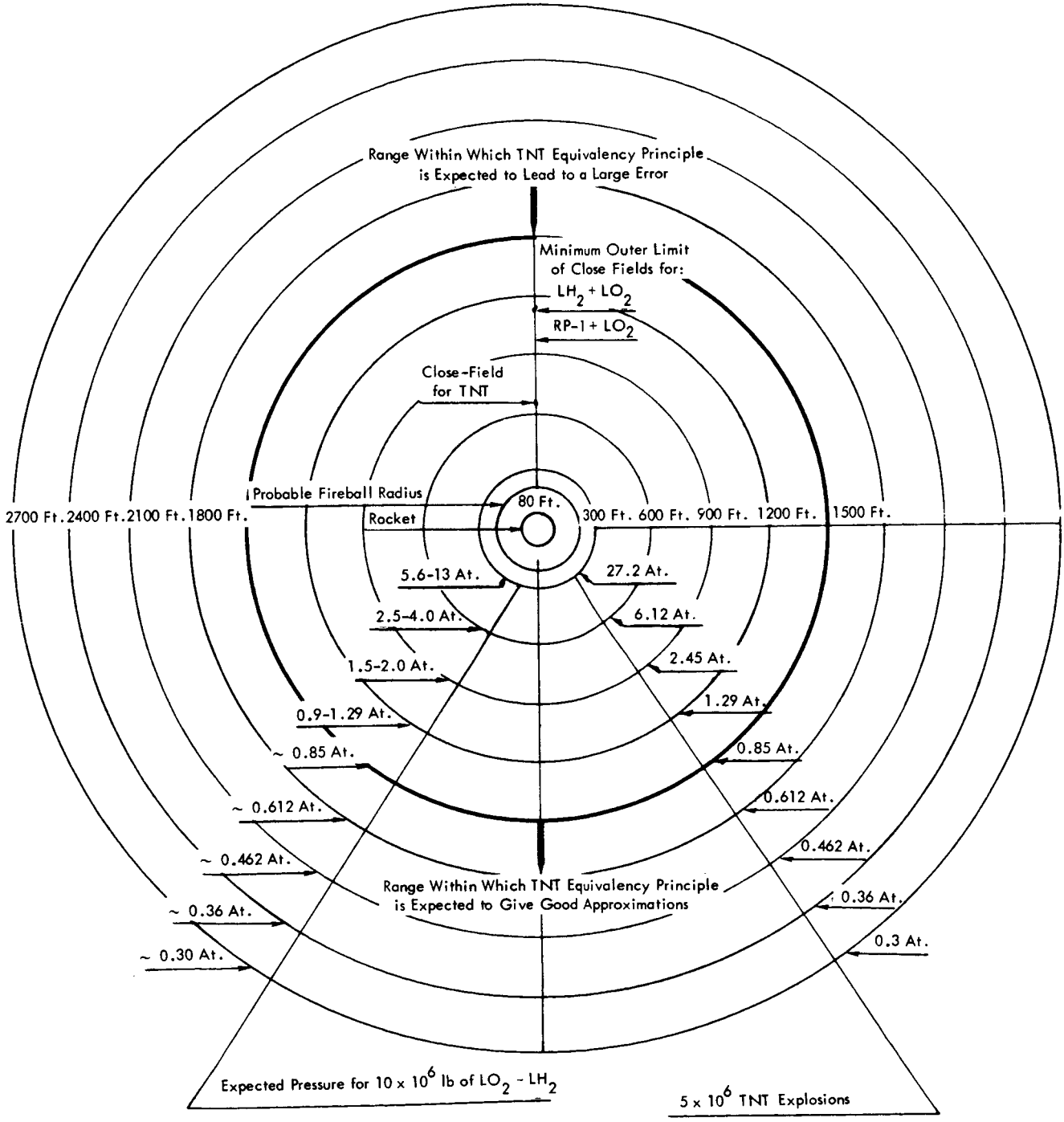

Figure 4: Close-Field for 5×10^6 lb. TNT Explosion Compared with Close-Field for Equivalent $LH_2 + LO_2$, and $RP-1 + LO_2$ Propellant Explosions

1.5 The Three Fields: Close, Medium and Far Field

The integration of the Navier-Stokes equations has given satisfactory results for TNT explosions. If a similar integration had been carried out for rocket explosions, there would be no need of differentiating between the close- and far-field. This need arises because TNT charts have to be used for predicting rocket explosions. Yet even if the proper calculations were available, damage criteria would suggest that the blast field actually be divided into three parts. From experimental results it is found that for peak overpressures less than 1 psi, only moderate damage will be suffered by life supporting structures. For peak overpressures greater than 1 psi but less than 10 psi, reinforcement of usual structures is possible. Only blast resistant designed structures will withstand peak overpressures greater than 10 psi. These conclusions are valid only for free air explosions of total effective energy smaller than, or equal to, approximately 20×10^6 lb of TNT, or for surface explosions of 10×10^6 lb of TNT, (see Appendix E). Moreover, for peak overpressures less than approximately 1.4 psi, very simple shock wave time history profiles can be used for structural response considerations (see Appendix D). Combining the above damage considerations with the previous physical arguments, the far-field is defined as the region where the peak overpressure is less than 1.47 psi, and charts for this region are given in Section 4. In the region where the peak overpressure is greater than 1.47 psi but less than 14.7 psi, TNT charts can be used for rocket explosion predictions where the energy involved may be as high as 5×10^6 lb of TNT (far-field equivalency). The results will be, at most, slightly conservative. This region, herein called the "medium field", is considered in the present report and charts for it are given in Section 4. The region in which the pressure is greater than 14.7 psi is of interest only for blast resistant structures and economical predictions of blast loads can not be made by the TNT charts. An accurate treatment of this region, previously defined as the close-field, is omitted from the present report and postponed to a later one. Nevertheless, it is possible for the reader to use the charts for the medium-field, for close-field estimates, if over conservative design is acceptable, or Figure 3 if more realistic tentative figures are preferable.

Finally, in Appendix C, the blast equations, as they have been used during the past 20 years of research on blast problems, are given along with their derivations from the basic Navier-Stokes equations and relative assumptions. Also, in Appendix C, some considerations on the scaling laws are presented and these considerations further discourage the use of TNT charts for close-field computations for rocket explosions.

2.0 EXPLOSION ENERGY AND BLAST SCALING LAWS

The charts which are given in Section 4 for the calculations of the blast parameters are entered with far-field TNT equivalencies using scaling laws. It is therefore necessary to define both far-field TNT equivalencies, and scaling laws, and their ranges of applications. These relationships are simply defined in the present section. Detailed explanations are given in the Introduction and in the Appendices.

It has been experimentally observed that, far from the explosion site, the air shock assumes a form depending only on the energy of the explosion. In turn, the energy of any explosion is commonly measured in terms of the weight of a given explosive whose explosion energy is known. TNT explosive which releases 252.28 Kcal/mole or 1.51×10^6 ft. lb/lb_{TNT}, is currently used as the energy unit for explosions. To stress the fact that only far from the explosion site is the air shock dependent solely on the energy, the TNT equivalencies are herein called "far-field-TNT-equivalencies". This definition is also consistent with the fact that far-field measurements are actually used to determine the explosive energy of a charge.

It has also been observed that distances, for a given peak overpressure, scale with the cube root of the energy or, if preferred, with the cube root of the far-field-TNT-equivalency. Thus, on the principle of energy as the leading factor we can write:

$$\frac{d}{d_r} = \frac{h}{h_r} = \frac{WT^{1/3}}{WT_r^{1/3}}$$

These scaling laws state that: For a given overpressure, the distance from the explosion (d), and explosion altitude (h) are proportional to the cube root of the explosion energy (WT). Cube root scaling can also be applied to arrival time, phase durations, and impulse provided that the distances are first scaled according to the cube root law. With this understanding it is possible to write:

$$\begin{cases} \dfrac{d}{d_r} = \dfrac{WT^{1/3}}{WT_r^{1/3}} \\ \\ \dfrac{t_p^+}{t_{p_r}^+} = \dfrac{WT^{1/3}}{WT_r^{1/3}} \end{cases} \quad \text{and} \quad \begin{cases} \dfrac{d}{d_r} = \dfrac{WT^{1/3}}{WT_r^{1/3}} \\ \\ \dfrac{I_p^+}{I_{p_r}^+} = \dfrac{WT^{1/3}}{WT_r^{1/3}} \end{cases}$$

The numerical examples of Section 4 will help in understanding the use of the above expressions.

Therefore, for a given reference explosion energy (WT_r), if distances (d_r), explosion altitudes (h_r), impulses $\left(\frac{I^+}{p}\right)_r$ and time durations (t_r) are known as functions of peak overpressures, the corresponding values for a different explosion energy can be readily computed. Charts for peak overpressure smaller than 14.7 psi (Section 4) are based on this principle.

There are several limitations to both far-field-TNT-equivalency and application of the above scaling laws. Some of these limitations are more theoretical than practical. However, one practical limitation has to be clearly restated: Neither the far-field-TNT-equivalencies nor the energy scaling laws hold when the close-field of an explosion is considered. As stated earlier, the main reason for this is that the energy is no longer the only important parameter.

Table I gives far-field TNT equivalencies for both solid and liquid propellants suggested by Reference 4. We might anticipate that even for peak overpressure less than 14.7 psi the equivalencies of Table I lead to conservative estimates for large rockets but, at present, this last safety margin has to be accepted. Determination of less conservative values for far-field-TNT-equivalencies must await the completion of experimental test programs such as the one being carried out at Edwards Air Force Base under sponsorship by NASA, Marshall Space Flight Center.* It is also to be noted, that while in the present report explicit consideration has been given to liquid propellants, the charts presented here can be used also for solid propellants since for peak overpressures less than 14.7 psi the TNT equivalent is the only necessary parameter. Finally, in using the charts of the present report, attention must be paid to the fact that loaded rockets on the launching pad or in flight are the main objects of the present study. Hence, the charts of this report can also be used for stage tests where a rocket partially or completely loaded is tested far from storage areas and not connected with them. For engine tests further elements must be considered. During an engine test the propellants are generally fed from storage areas through pipes while the test is in process. In this case the propellant in the pipes should be considered as well as the possible delay between an initial explosion and the actual shut-down of the feeding system. Experience shows that this time is relevant. Extension of a possible explosion in the testing area to the storage areas and vice versa must also be considered. For these and other storage problems, the specifications given in Reference 4 are recommended.

* August, 1965. A fully fueled Saturn S-4 has been intentionally exploded at Edwards Air Force Base, California. A total of 74,000 lb of LO_2 and 16,000 lb of LH_2 has given a far-field-TNT-equivalency of only 9,000 lb, (10 percent).

TABLE I

LIQUID PROPELLANT EXPLOSIVE (FAR FIELD) EQUIVALENCIES

Propellant Combination	Static Test Stands	Range Launch Pads
LO_2 - LH_2	60%	60%
LO_2 - LH_2 + RP-1	Sum of (60% for LO_2 - LH_2; 10% for LO_2 - RP-1)	Sum of (60% for LO_2 - LH_2; 20% for LO_2 - RP-1)
LO_2 - RP-1 or LO_2 - NH_3	10%	20% up to 500,000 pounds plus 10% over 500,000 pounds
IRFNA - Aniline*	10%	10%
IRFNA - UDMH*	10%	10%
IRFNA - UDMH + JP-4*	10%	10%
N_2O_4 - UDMH + N_2H_4*	5%	10%
N_2O_4 - UDMH + N_2H_4 - Solid*	5% plus the explosive equivalent of the solid propellant	10% plus the explosive equivalent of the solid propellant
Tetranitromethane (alone or in combination)	100%	100%
Nitromethane (alone or in combination	100%	100%

* These are hypergolic combinations.

Basis: Recommendations of ASESB Work Group on Explosive Equivalents for Liquid Propellants. Tetranitromethane and nitromethane are known to be detonable.

NOTES:
1. The percentage factors to be used to determine the explosive equivalencies of propellant mixtures at launch pads and static test stands when such propellants are located aboveground and are unconfined except for their tankage. Any configurations other than stated above should be considered on an individual basis to determine the equivalencies.
2. The equivalencies of any non-nuclear explosives will be added to the above equivalencies.
3. The above values were obtained from Reference 4.

3.0 EXPLOSION ENERGIES FOR POSSIBLE FUTURE VEHICLE CONFIGURATIONS

It is useful to list briefly the configurations which might be characteristic of future chemical rockets in order to determine the order of magnitude of the energy which might be released in an accidental explosion. For this purpose data on 19 rocket configurations have been grouped in Table II. From the current Saturn V (7.5×10^6 lb of thrust) to the advanced LH_2 - LO_2 configurations (30×10^6 lb of thrust), the explosive energy is seen to increase from 1.76×10^{12} ft. lb. (1.167×10^6 far-field-TNT-equivalent) to 18.9×10^{12} ft. lb. (12.53×10^6 far-field-TNT-equivalent) which means that the peak overpressure might, in the future, be 10 times what is presently expected from a Saturn V explosion. However, the far-field-TNT-equivalencies of Table II were calculated using the propellant percentages suggested by Reference 4 (Table I) and it is felt that these percentages are conservative for large rockets since they are based on small propellant explosion tests where most of the propellant actually explodes simultaneously. Thus, it is believed that a 5×10^6 lb. far-field-TNT-equivalency can be considered reasonable for the largest of the above future vehicles. On the other hand the reader is cautioned to use the D.O.D. specifications in Reference 4 until they have been officially superseded. A 5×10^6 lb TNT equivalent explosion is then chosen to carry out sample calculations which can be repeated for every chosen TNT equivalency. Table II also includes maximum chemical energy available and mechanical energy. The maximum chemical energies are the top values of both mechanical and explosive energies. The chemical energies are based on heats of combustion of 51,500 Btu/lb for H_2 and 18,500 Btu/lb for RP-1. It would have been more accurate to choose about 40,000 and 16,000 Btu/lb, respectively, to take into account the fact that the mixture ratios actually used are not stoichiometric. The mechanical energy is herein defined as the total kinetic energy of the exhaust gases estimated by $WT\ (V_e^2/2g)$ where WT is the propellant weight, V_e the exit velocity, and g is the acceleration of gravity.

TABLE II: FUTURE VEHICLE CONFIGURATIONS

No.	NASA Ident. **	Liftoff Thrust (Lb. x 10^6)	Liftoff Weight (Lb. x 10^6)	Total Length (Ft.)	Maximum Diameter (Ft.)	No. of Stages
1	SATURN V	7.5	--	361	33	3
2	V-1 (70)	9.0	--	410	33	--
3	V-1 (70)	9.0	--	384	33	3
4	V-2 (72)	9.0	--	398	33	3
5	V-3 (75)	9.0	--	410	33	3
6	V-3 (75)	9.0	--	410	33	--
7	V-4	7.5	--	336	55	3
8	1B	25.2	20.11	415	65.5	3
9	B	28.8	23.00	349	67.5	3
10	F-1	30.0	24.00	343	72	3
11	1C	32.4	25.20	454	69	3
12	24G	18.0	14.40	386	70.5	3
13	34	30.0	24.00	406	90	2
14	H	24.3	19.4	365	78	2
15	33	30.2	24.20	377	80	2
16	14B	37.64	26.85	452	60	3
17	14A	47.05	33.67	507	62	3
18	T65G	54.9	38.10	535	70	3
19	$E2_{SR}$	44.0	31.40	303	123	3

* Data of configurations 1 through 7 from personal communication with R. Jewell,
** Chief of Advanced Methods and Research Section, P and VE, M.S.F.C., Huntsville, Alabama. Data of configurations 8 through 19, from: J. Young and J. Heindrichs: Structural Dynamics Conceptual Design, Part I, Martin Co., Report NOVA, TN-19.

TABLE II: FIRST STAGES (Continued)

No.	Propellant Type and Weight		Mixture Ratio	Total Prop WT	Engine No. and Type	Exit * Velocity	Max.** Chemical	Total Mech. E	TNT Equivalent
	Lbx10^6	Lbx10^6	* * * *	Lbx10^6		Ft/Sec	Lb. Ft x 10^{12}	Lb · Ft x 10^{12}	(Lb x10^6)
1	3.2 *a	1.42*b	2.25:1*	4.62	5 F-1	9,300	20.4	6.2	.462
2	3.74*a	1.66*b	2.25:1*	5.40	5 F-1A	10,200	23.9	8.72	.54
3	3.74*a	1.66*b	2.25:1*	5.40	5 F-1A	10,200	23.9	8.72	.54
4	3.74*a	1.66*b	2.25:1*	5.40	5 F-1A	10,200	23.9	8.72	.54
5	3.74*a	1.66*b	2.25:1*	5.40	5 F-1A	10,200	23.9	8.72	.54
6	3.74*a	1.66*b	2.25:1*	5.40	5 F-1A	10,200	23.9	8.72	.54
7	3.05*a	1.35*b	2.25:1*	4.40	5 F-1A	10,200	19.4	7.1	.44
8	10.54a	4.68b	2.25:1	15.22	14 F-1A	10,200	67.5	24.6	1.522
9	12.7a	5.8b	2.25:1	18.50	16 F-1A	10,200	83.5	30.0	1.850
10	12.6a	5.7b	2.25:1	18.30	4 L7.5	10,200	82.0	29.5	1.830
11	12.91a	5.74b	2.25:1	18.65	18 F-1A	10,200	82.5	30.1	1.864
12	9.08a	1.3c	7:1	10.38	18 HP-1	12,300	52.0	24.4	6.22
13	18.3a	2.6c	7:1	20.9	5 L6H	12,500	104.0	50.9	12.5
14	14.32a	2.88c	5:1	17.2	1 L4-3H 4 L5.0H	12,500	115.0	41.9	10.3
15	18.6a	2.7c	7:1	21.3	24 HP-1	12,300	108.0	50.2	12.8
16	——	SOLID	——	19.0	4 280"	8,500	——	21.4	3.8
17	——	SOLID	——	24.0	4 300"	8,500	——	27.0	4.8
18	——	SOLID	——	25.0	6 260"	8,500	——	28.1	5.0
19	——	SOLID	——	21.0	4 300"	8,500	——	23.6	4.2

* Theoretical Value, the effective value being unknown.

a = LOX

b = RP-1

c = LH_2

* * Based on 18,500 Btu/lb for RP-1; 51,500 Btu/lb for H_2.

* * * * The mixture ratio is not necessarily equal to the ratio of the propellant weights.

TABLE II: SECOND STAGES (Continued)

No.	Propellant Type and Weight		Mixture Ratio	Total Prop WT	Engine No. and Type	Exit * Velocity	Max.* * Chem.E	Total Mech.E	TNT Equivalent
	Lb x 10^6	Lb x 10^6	* * * *	Lb x 10^6		Ft/sec	Lb Ft x 10^{12}	Lb Ft x 10^6	Lb x 10^6
1	.7825*a	.1565*c	5:1*	.939	5 J-2	12,500*	6.25	2.28	.563
2	.8335*a	.1665*c	5:1*	1.0	5 J-2	12,500*	6.66	2.43	.6
3	.8335*a	.1665*c	5:1*	1.0	5 J-2	12,500*	6.66	2.43	.6
4	.8335*a	.1665*c	5:1*	1.0	5 J-2	12,500*	6.66	2.43	.6
5	1.0*a	.2*c	5:1*	1.2	5 .315M-1	12,500*	8.0	2.92	.72
6	1.0*a	.2*c	5:1*	1.2	5 .315M-1	12,500*	8.0	2.92	.72
7	1.0* a	.2*c	5:1*	1.2	5 J-2	12,500*	8.0	2.92	.563
8	2.093 a	.418 c	5:1	2.51	2 M-1B	12,500*	16.72	6.1	1.51
9	1.9 a	.388 c	5:1	2.29	2 M-1	12,500*	15.5	5.55	1.37
10	2.7 a	.65 c	5:1	3.35	3 M-1	12,500*	26.0	8.12	2.01
11	2.938 a	.587 c	5:1	3.53	3 M-1B	12,500*	23.5	8.55	2.12
12	1.4 a	.206 c	7:1	1.6	2 HP-1	12,300*	8.24	3.76	.94
13	--	--	--	--	--	--	--	--	--
14	--	--	--	--	--	--	--	--	--
15	--	--	--	--	--	--	--	--	--
16	3.812 a	.763 c	5:1	4.58	4 M-1	12,500*	30.5	11.1	2.74
17	4.63 a	.926 c	5:1	5.56	5 M-1	12,500*	37.0	13.5	3.34
18	6.85 a	1.37 c	5:1	8.22	5 M-1	12,500*	54.8	20.0	4.92
19	5.2 a	1.1 c	5:1	6.30	2 L-4H	12,500*	44.0	15.3	3.78

* Theoretical value, the effective value being unknown.

* * Based on 18,500 Btu/lb for RP-1; 51,500 Btu/lb for H_2.

* * * * The mixture ratio is not necessarily equal to the ratio of the propellant weights.

a = LOX

c = LH_2

TABLE II: THIRD STAGES (Continued)

No. of Units	Propellant Type and Weight		Mixture Ratio	Total Prop. WT	Engine No. and Type	Exit * Velocity	Max.** Chem. E.	Total Mech. E	TNT Equivalent
	Lb x 10^6	Lb x 10^6	* * * *	Lb x 10^6		Ft/Sec	Lb Ft x 10^{12}	Lb Ft x 10^6	Lb x 10^6
1	.1976*a	.0394*c	5:1*	.237	- -	12,500*	1.575	.576	.142
2	- -	- -	- -	- -	- -	- -	- -	- -	- -
3	.192*a	.038*c	5:1*	.230	1 J-2	12,500*	1.52	.560	.138
4	.292*a	.058*c	5:1*	.350	1 RL-20	12,500*	2.32	.850	.21
5	.292*a	.058*c	5:1*	.350	1 RL-20P3	12,500*	2.32	.850	.21
6	- -	- -	- -	- -	- -	- -	- -	- -	- -
7	.292*a	.058*c	5:1*	.350	1 RL-20P3	12,500*	2.32	.850	.21
8	.039 a	.008 c	5:1	.047	6 LR-115	12,500*	.32	.114	.0282
9	.037 d	.0206 c	1.8:1	.0576	4 T-20K	- -	- -	- -	- -
10	.037 d	.0206 c	1.8:1	.0576	4 T-20K	- -	- -	- -	- -
11	.05 a	.01 c	5:1	.06	6 LR-115	12,500*	.4	.146	.036
12	.05 a	.01 c	5:1	.06	6 LR-115	12,500*	.4	.146	.036
13	.05 a	.01 c	5:1	.06	6 LR-115	12,500*	.4	.146	.036
14	.037 d	.0206 c	1.8:1	.0576	4 T-20K	- -	- -	- -	- -
15	.05 a	.01 c	5:1	.060	6 LR-115	12,500*	.4	.146	.036
16	.04 a	.008 c	5:1	.048	6 LR-115	12,500*	.32	.117	.0282
17	.05 a	.01 c	5:1	.06	6 LR-115	12,500*	.4	.146	.036
18	.0485 d	.027 e	1.8:1	.0755	2 T-20K	- -	- -	- -	- -
19	.037 d	.0206 e	1.8:1	.0576	4 T-20K	- -	- -	- -	- -

* Theoretical value, the effective value being unknown.

* * Based on 18,500 Btu/lb for RP-1; 51,500 Btu/lb for H_2

* * * * The mixture ratio is not necessarily equal to the ratio of the propellant weights.

a = LOX

c = LH_2

d = $N_2 O_4$

e = Aerozine

TABLE II (Continued)

TOTALS

No.	Maximum Chemical Energy	Mechanical Energy	TNT *** Equivalent	
	Lb Ft x 10^{12}	Lb Ft x 10^{12}	Lb Ft x 10^{12}	Lb x 10^{6} TNT
1	28.225	9.056	1.76	1.167
2	30.56	11.15	1.72	1.140
3	32.08	11.71	1.93	1.278
4	32.88	12.00	2.04	1.350
5	34.22	12.49	2.22	1.470
6	31.90	11.64	1.90	1.260
7	29.72	10.87	1.83	1.213
8	84.54	30.81	4.62	3.060
9	~99.00	~35.55	4.86	~3.220
10	~108.00	~37.62	5.80	~3.840
11	~106.40	38.80	6.07	4.020
12	60.64	28.31	10.85	7.196
13	104.40	51.05	18.90	12.536
14	~115.00	~41.90	15.55	~10.300
15	108.40	50.35	19.40	12.830
16	- -	32.62	9.90	6.568
17	- -	40.65	12.30	8.176
18	- -	~48.10	14.90	~9.920
19	- -	~38.90	12.05	~7.980

*** TNT equivalencies in Lb Ft are equal to TNT equivalencies in Lb TNT times 1.5×10^{6}.

4.0 DESIGN CHARTS AND EXAMPLES

It has been shown that for rocket explosions with far-field-TNT-equivalences of the order of 10^6 lb., different criteria and approximations have to be used for different peak overpressure ranges. From the physics of the blast and from damage criteria for explosions of this order of energy, three ranges are found to be suited for the different approaches:

Far-Field:	Peak overpressure	$\leq$ 1.47 psi
Medium-Field:	Peak overpressure	$\geq$ 1.47 psi and $\leq$ 14.7 psi
Close-Field:	Peak overpressure	$\geq$ 14.7 psi

In the present section, charts and numerical examples are given for the far-and medium-field. Charts and examples for the close-field will be presented in a later report. The charts for the medium-field can be used for the close-field as well, but the results are believed to be very conservative. It is important to note that a 1 kiloton TNT surface explosion is equal to a 2 kiloton nuclear surface explosion because the energy of the nuclear explosion refers to the total energy, 50 percent of which is estimated to be transferred to the air shock; the remaining 50 percent being thermal radiation (35 percent), residual nuclear radiation (10 percent), and initial nuclear radiation (5 percent).

For the sake of clarity, the following scheme will be followed within each of the two regions:

- Definition of the parameter
- Figure from which the parameter can be read
- Reliability of the figure *
- Short Comments
- Numerical examples

All the numerical instances are for a 5×10^6 lb. farfield-TNT-equivalent rocket explosion. For this explosion, overpressure and dynamic pressure time variations are calculated at distances where the peak overpressure would be:

0.0147 psi (Section 4.1)
1.47 psi (Section 4.2)
14.7 psi (Section 4.2)

Results are then summarized in Table III. These results are expected to be conservative,

* Unless otherwise stated, the reliability of each figure comes from Reference 8.

even for the largest chemical rockets of the foreseeable future (up to 40×10^6 lb of thrust).

The number of significant figures used in the present section are not always consistent with the approximations implied in the theory. Nevertheless, they are kept to help the reader to follow the problems which generally are related with each other and to avoid large errors at the end of the chain-calculations. It is left to the reader to round off the numbers.

4.1 Rocket Explosion Air Blast Parameters for Peak Overpressures $\leqslant$ 1.47 psi

4.1.1 Peak Overpressure: p_s

Figure 5 can be used. *

Reliability: Peak overpressure from Figure 5 is reliable to $\pm$ 20 percent and slant distance to $\pm$ 17 percent for overpressures smaller than 1.47 psi.

Comments: The reliability limits are sufficient to take into account effects of inflight explosion but not possible focusing due to weather conditions.

Example:

Given - A far-field-TNT-equivalency of 5×10^6 lb (WT).

Find - The slant distance at which the peak overpressure (p_s) would be $\leqslant$ 0.0147 psi.

Solution - From Figure 5 the reference distance, d_r, can be found knowing the peak overpressure (p_s); thus, $d_r \geqslant 140 \times 10^3$ ft.

Applying the scaling laws (Sec. 2.0):

$$d \geqslant d_r \left[(WT)/WT_r \right]^{1/3} = 240 \times 10^3 \text{ ft.}$$

Considering the reliability of Figure 5 ($\pm$ 17 percent):

$$d \geqslant (240 \pm 40.8)\, 10^3 \text{ ft.}$$

This value of d can be used for both ground and inflight explosion.

---

* From Reference 13.

4.1.2 Peak Dynamic Pressure: q_s

The peak dynamic pressure is neglible for $p_s < 1.47$ psi (See Appendix D). Nevertheless, if it is desired, Figure 11 in Section 4.2.2 could be used. In this case, see Section 4.2.2 for examples.

4.1.3 Durations of Positive Phases: t_p^+ and t_q^+

Figure 13 can be used.

Reliability: Time durations from Figure 13 are reliable to ± 10 percent.

Comments: For overpressure $\leqslant 1.47$ psi, the dynamic pressure can be neglected (see Appendix D). Hence, its positive phase duration need not be calculated. The reference overpressure positive phase duration can be assumed to have a constant value of 0.45 ±0.045 sec.

Example:

Given - A far-field TNT equivalency of 5×10^6 lb (WT).

Find - The duration of the positive overpressure phase (t_p^+) at a slant distance of 240×10^3 ft. (the peak overpressure at that distance would be 0.0147 ± 0.0029 psi).

Solution - The reference overpressure phase duration is equal to 0.45 sec. Thus, applying the scaling laws, (Section 2.0) we have:

$$t_p^+ = (t_p^+)_r \, (WT/WT_r)^{1/3} = 0.780 \text{ sec.}$$

Considering the reliability of the reference value:

$$t_p^+ = (0.780 \pm 0.078) \text{ sec.}$$

4.1.4 Time Variations of Overpressure and Dynamic Pressure

For overpressure $\leqslant 1.47$ psi, the overpressure can be assumed to vary linearly from its peak value to zero at the end of the positive phase duration.

Example:

Given - A far-field-TNT-equivalent of 5×10^6 lb (WT).

Find - The time variation of overpressure at a slant distance of 240×10^3 ft (where the peak overpressure would be 0.0147 ± 0.0029 psi).

Solution - From the results of Section 4.1.1 and 4.1.3 the following sawtooth time histories can be drawn:

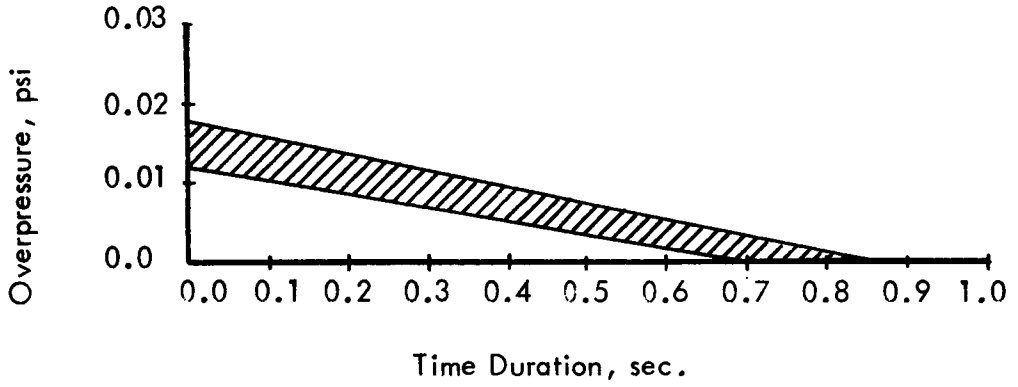

Any curve in the calculated range is a possible solution.

4.2 Rocket Explosion Air Blast Parameters for Peak Overpressures $\geq$ 1.47 but $\leqslant$ 14.7 psi

Within the peak overpressure range of 1.47 to 14.7 psi, the physical differences between air blast from rocket explosions and TNT are expected to be detectable. Nevertheless, for far-field-TNT-equivalencies of the order of 5×10^6 lb, these differences are not going to be any larger than those possibly produced by secondary effects and can be considered falling within the reliability limit of the TNT curves themselves. On the other hand, neither complete experimental data nor proper theoretical calculations on rocket explosion air blasts are presently available. Hence, it is felt that within this range of peak overpressures, the use of TNT air blast charts to predict rocket explosion air blast parameters has to be considered a necessary and justified compromise.

The charts of the present section summarize works of Bethe, H. A.; Fuchs, K.; Peierls, E. R.; Von Neumann, J.; Brinkley, S. R.; Kirkwood, J. G.; Brode, H. L.; Courant, R.; Friedrichs, K. O.; Taylor, G. I.; et al. In particular, Figures 6, 7, 8, 9, 11, 12, and 14 are from Reference 8.

4.2.1 Peak Overpressure: p_s

Figures 5 through 9 can be used.

Reliability: Peak overpressures and distances from Figure 5 are reliable to $\pm$ 10 percent for overpressures between 14.7 and 1.47 psi. Peak overpressures from Figures 6, 7, 8, and 9 are reliable to $\pm$ 20 percent; distances to $\pm$ 17 percent.

Comments: In Figures 6, 7, 8, and 9, good surface conditions refer to ground conditions approaching the ideal reflecting ones, namely, ice, water or concrete surfaces. Average surface conditions refer to all other surface conditions.

Example:

(a) Given - A far-field-TNT-equivalency of 5×10^6 lb (WT) and assuming a ground explosion.

(a1) Find - The distance at which the peak overpressures would be $\lesssim$ 14.7 psi.

Solution - From Figure 5, the reference distance, d_r can be found knowing the peak overpressure, p_s; thus,

$$d_r \gtrsim 0.8 \times 10^3 \text{ ft.}$$

Applying the scaling laws (Section 2.0):

$$d = d_r (WT/WT_r)^{1/3} \gtrsim 1.37 \times 10^3 \text{ ft.}$$

Considering the reliability of Figure 5 ($\pm$ 10 percent):

$$d \gtrsim (1.37 + 0.137)\, 10^3 = 1.507 \times 10^3 \text{ ft.}$$

(a2) Find - The distance at which the peak overpressure, p_s, would be $\lesssim$ 1.47 psi. Repeating the procedure outlined in example (a1), it is found

$$d \gtrsim (5.810 + 0.581)\, 10^3 = 6.391 \times 10^3 \text{ ft.}$$

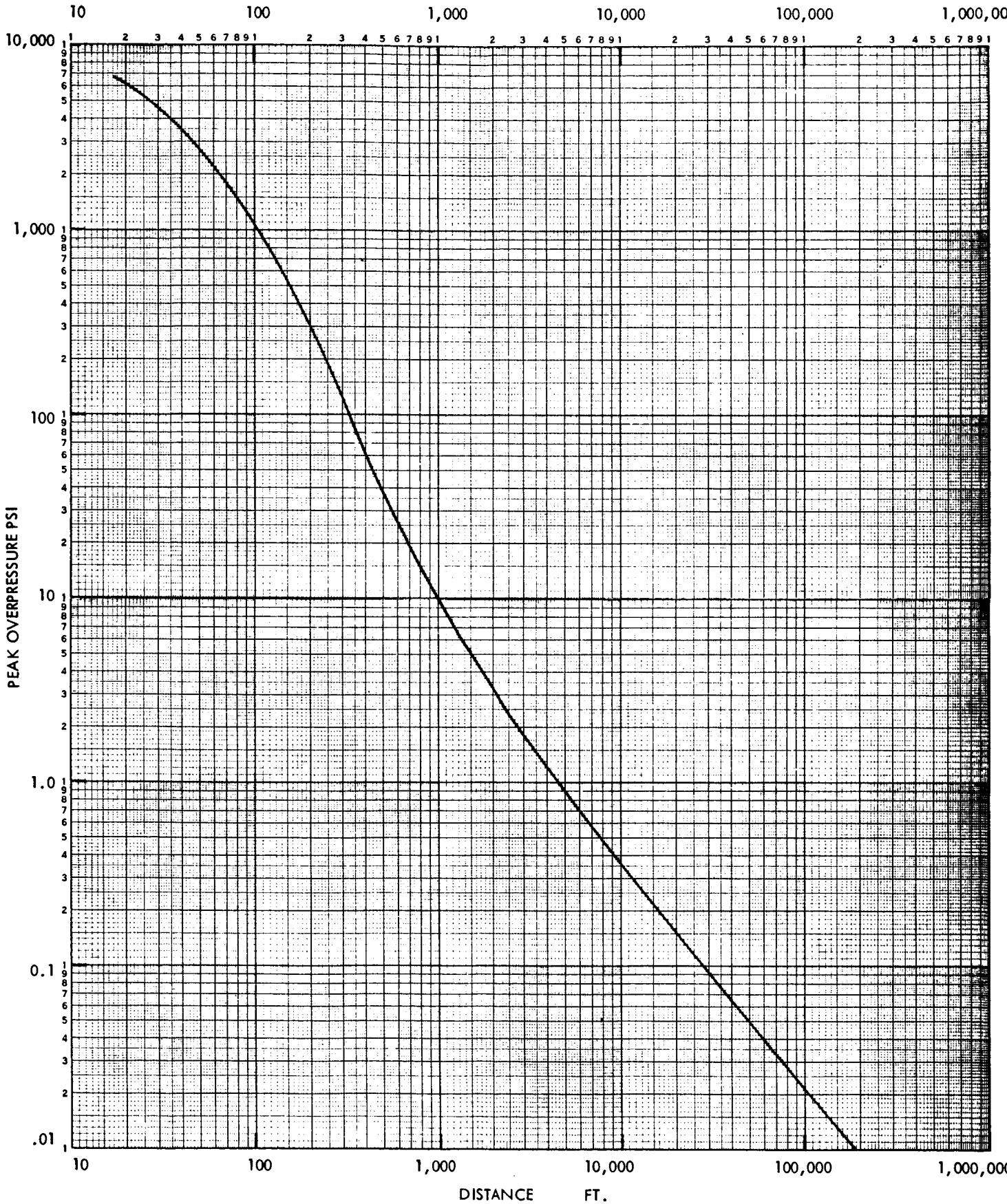

Figure 5: Peak Overpressure versus Distance for 10^6 lb T.N.T. Surface Explosion

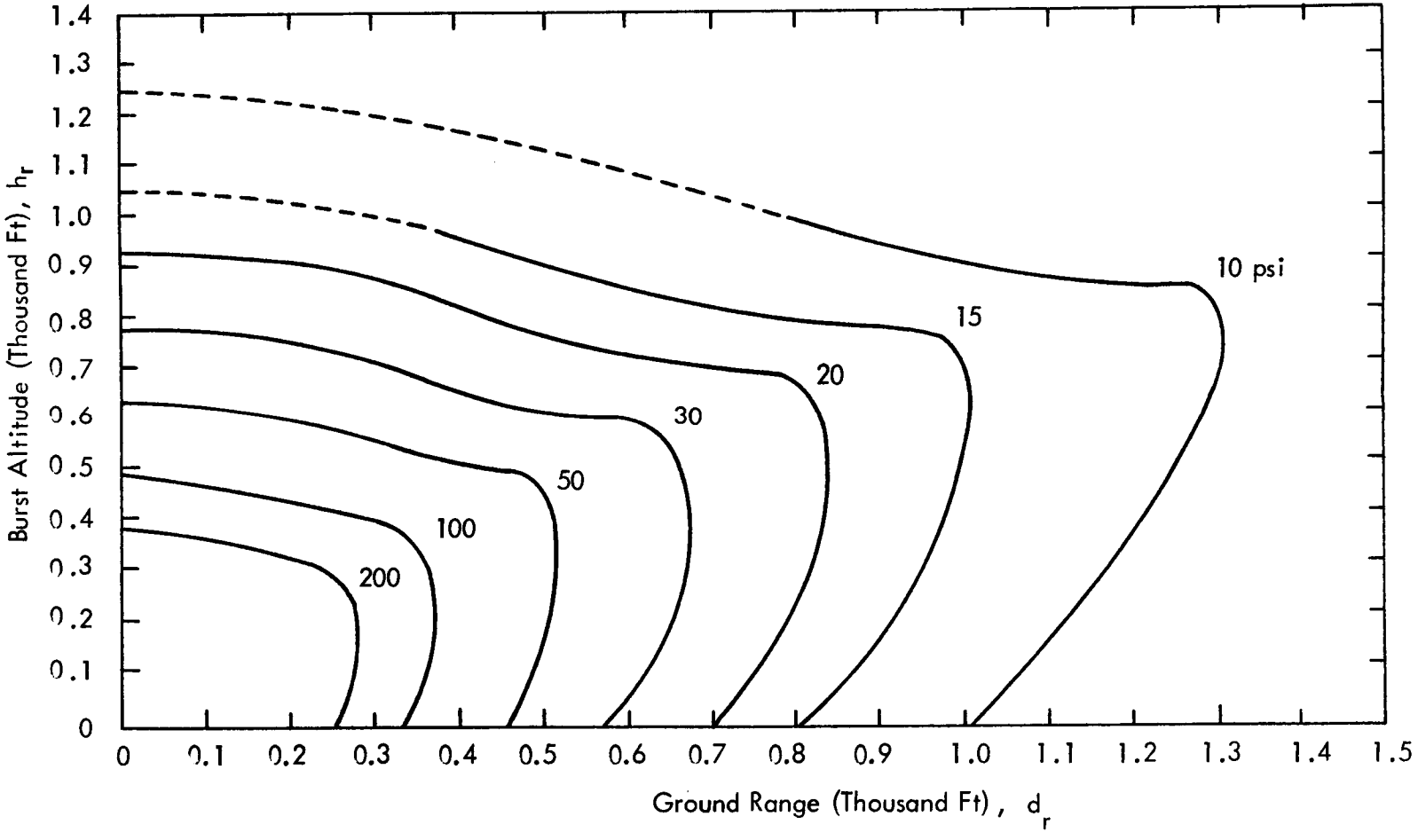

Figure 6. Peak Overpressure on the Surface as a Function of Burst Altitude and Ground Zero Distance; 10^6 lbs of TNT at Sea Level for Good Surface Conditions

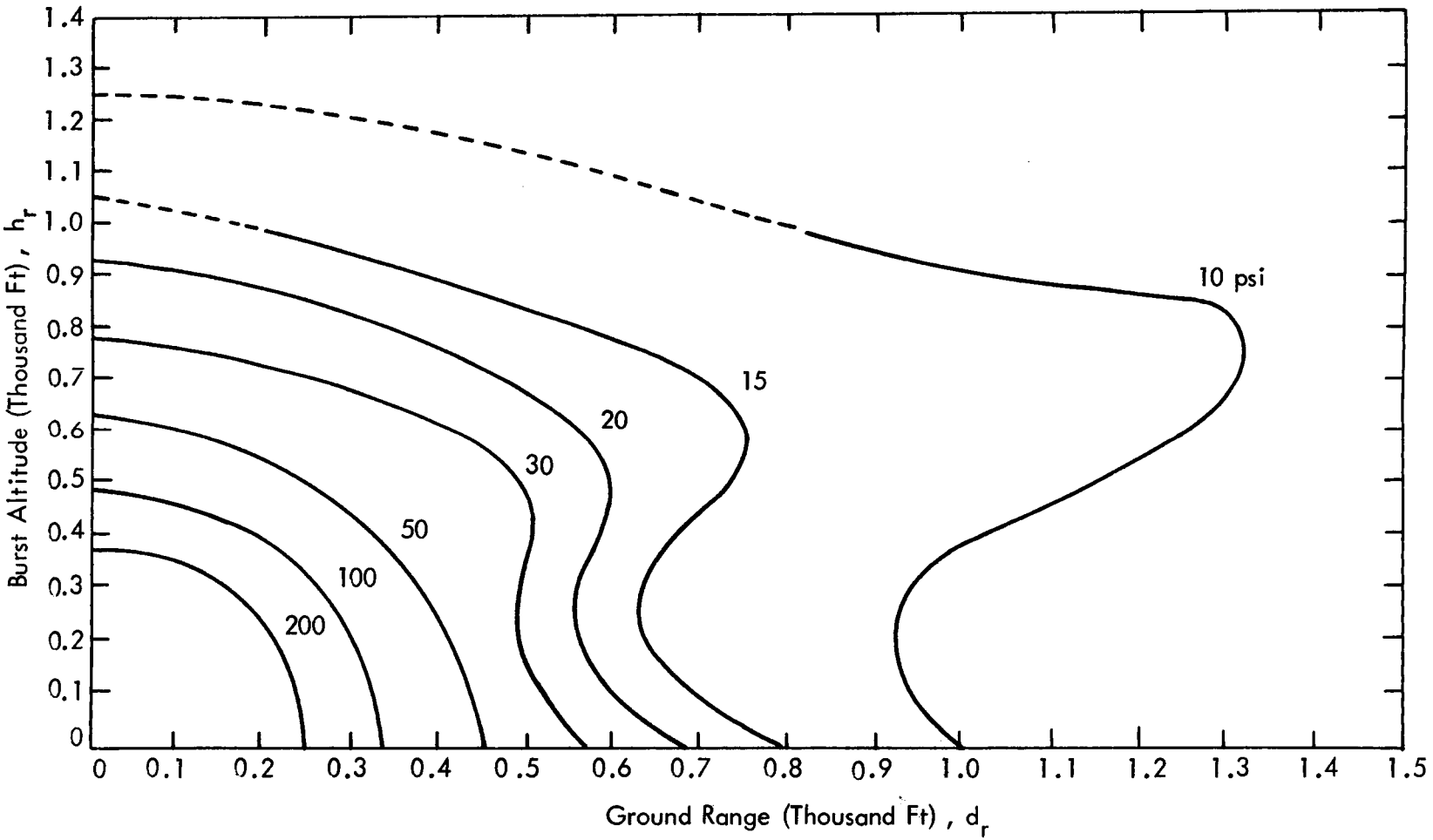

Figure 7. Peak Overpressure on the Surface as a Function of Burst Altitude and Ground Zero Distance; 10^6 lbs of TNT at Sea Level for Average Surface Conditions

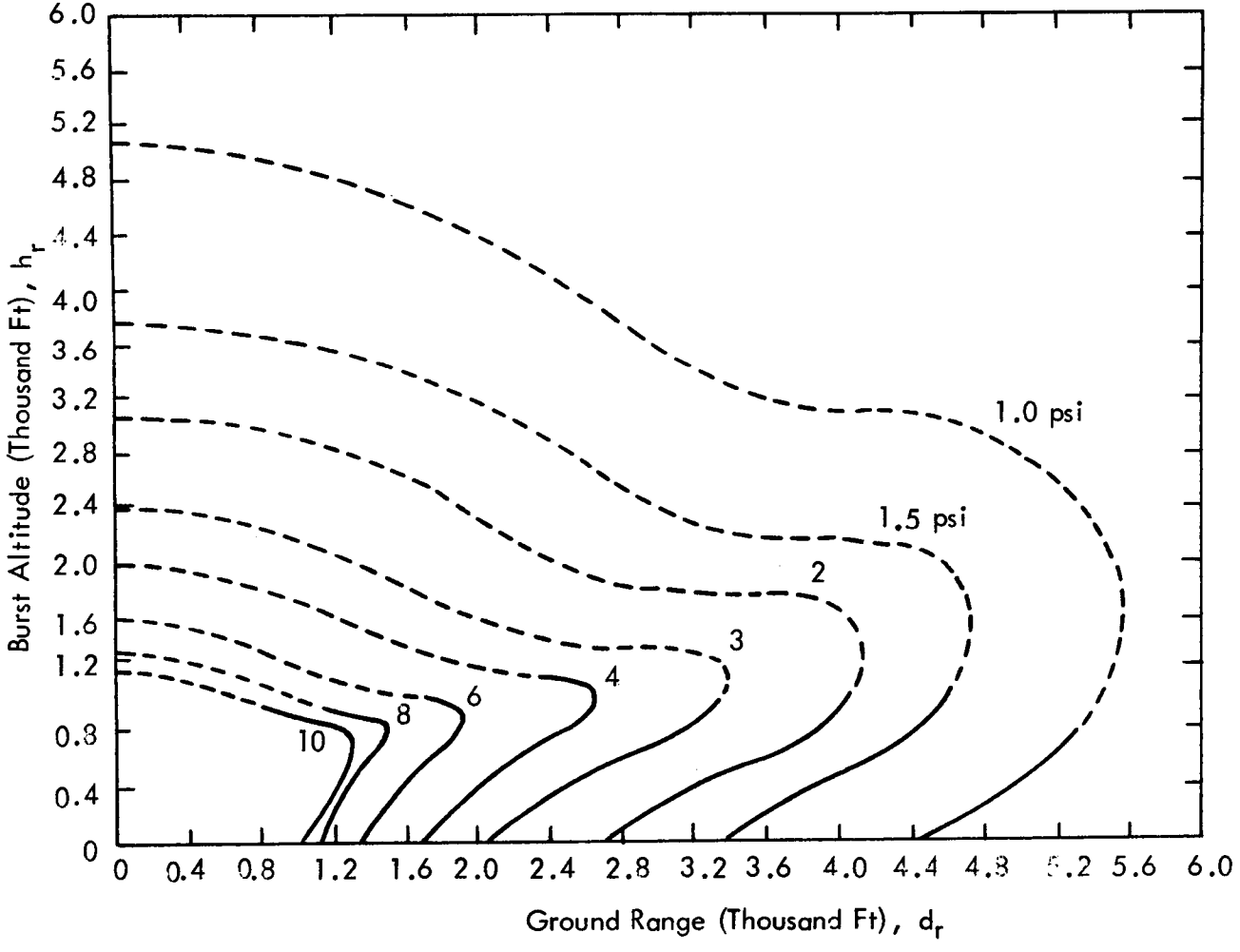

Figure 8. Peak Overpressure on the Surface as a Function of Burst Altitude and Ground Zero Distance; 10^6 lbs of TNT at Sea Level for Good Surface Conditions

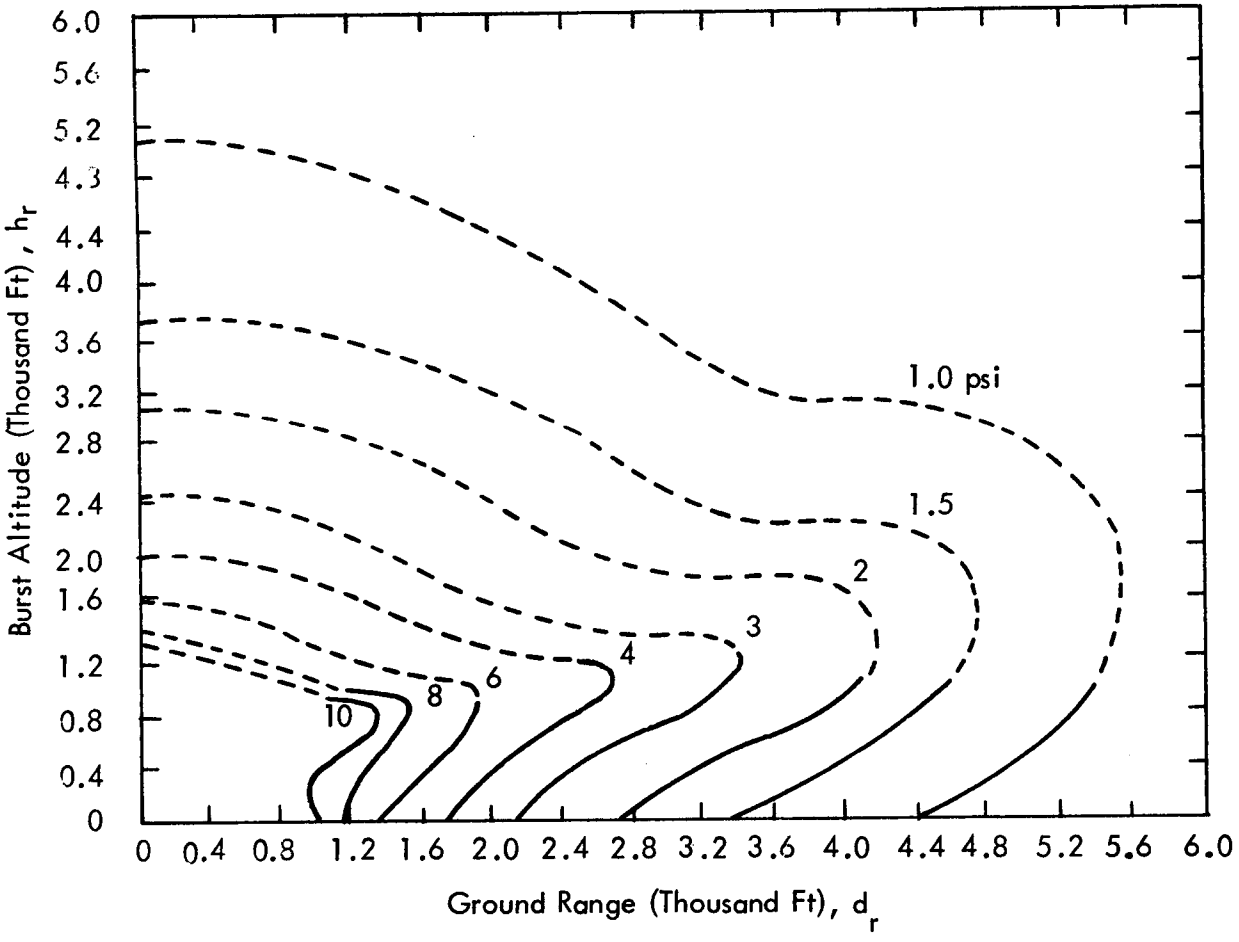

Figure 9. Peak Overpressure on the Surface as a Function of Burst Altitude and Ground Zero Distance; 10^6 lbs of TNT at Sea Level for Average Surface Conditions

(a3) Find - The peak overpressure at a distance of 5,810 ft.

Solution - From Figure 5, p_s can be found knowing d_r. Applying the scaling laws (Section 2.0), we have:

$$d_r = d\,(WT_r/WT)^{1/3} = 3.40 \times 10^3 \text{ ft.}$$

and from Figure 5

$$p_s = 1.4 \text{ psi}$$

Considering the reliability of Figure 5 ($\pm$ 10 percent):

$$p_s = 1.4 \pm 0.14 \text{ psi}$$

(b) Given - A far-field-TNT-equivalency of 5×10^6 lbs (WT)

(b1) Find - The distance from ground zero from which the peak overpressure would be $\leqslant$ 14.7 psi considering possible inflight explosions.

Solution - Define the surface conditions: To be conservative, assume good ground conditions. From Figure 6, interpolating between 10 and 15 psi, it is seen that the 14.7 psi line has a vertical tangent at about 1,020 ft. from ground zero and 500 to 800 ft. burst altitude. This means that a 10^6 lb. TNT explosion at an altitude of 500 to 700 ft. can give a peak overpressure of 14.7 psi or higher up to a maximum distance of 1,020 ft. Applying now the scaling laws, (Section 2.0):

$$h = h_r\,(WT/WT_r)^{1/3} = (0.85 \text{ to } 1.20)\,10^3 \text{ ft.}$$

$$d = d_r\,(WT/WT_r)^{1/3} = 1.74 \times 10^3 \text{ ft.}$$

Considering the reliability of Figure 6 (17 percent), the desired distance is

$$d = (1.74 + 0.296)\,10^3 = 2.04 \times 10^3 \text{ ft.}$$

for a blast altitude of 710 to 1,320 ft.

(b2) Find - The distance from ground zero from which the peak overpressure would be $\leqslant$ 1.47 psi considering possible inflight explosions.

Solution - Repeating the reasoning of the preceding solution, but using Figure 8, we now have

$$d_r = 4.80 \times 10^3 \text{ ft.} \qquad h_r = (1.40 \text{ to } 1.80)\ 10^3 \text{ ft.}$$

Applying now the scaling laws, (Section 2.0):

$$h = h_r\ (WT/WT_r)^{1/3} = (2.39 \text{ to } 3.08)\ 10^3 \text{ ft.}$$

$$d = d_r\ (WT/WT_r)^{1/3} = 8.20 \times 10^3 \text{ ft.}$$

Considering the reliability of Figure 8 (17 percent) the desired distance is:

$$d = (8.20 + 1.39)\ 10^3 = 9.59 \times 10^3 \text{ ft.}$$

for a blast altitude of

$$2{,}390 - 17 \text{ percent to } 3{,}080 + 17 \text{ percent} = 1{,}980 \text{ to } 3{,}600 \text{ ft.}$$

Notice that in the preceding instances, where surface blasts were assumed, the following corrected distances from ground zero were found:

For $p_s \leqslant 14.7$ psi, distance from ground zero $\geqslant$ 1,507 ft.

For $p_s \leqslant 1.47$ psi, distance from ground zero $\geqslant$ 6,391 ft.

while when inflight blasts are considered

For $p_s \leqslant 14.7$ psi, distance from ground zero $\geqslant$ 2,036 ft.

For $p_s \leqslant 1.47$ psi, distance from ground zero $\geqslant$ 9,590 ft.

Generally, the inflight blast condition is more critical than the surface blast condition and should be used in calculating possible load on buildings at launch sites. For overpressures smaller than 1.47 psi, the altitude effects become less significant and surface blast figures can be used. The reliability of calculated overpressures $\leqslant$ 1.47 psi are also less than the reliability of calculated overpressures from 14.7 to 1.47 psi (about 20 percent instead of about 10 percent) so that possible inflight explosions effects are already considered in the reliability limits.

4.2.2 Peak Dynamic Pressure: q_s

Figures 10, 11, and 12 can be used.

Reliability: Peak dynamic pressures from Figures 10, 11, and 12 are reliable to $\pm$ 25 percent for peak dynamic pressures $\leqslant$ 14.7 psi.

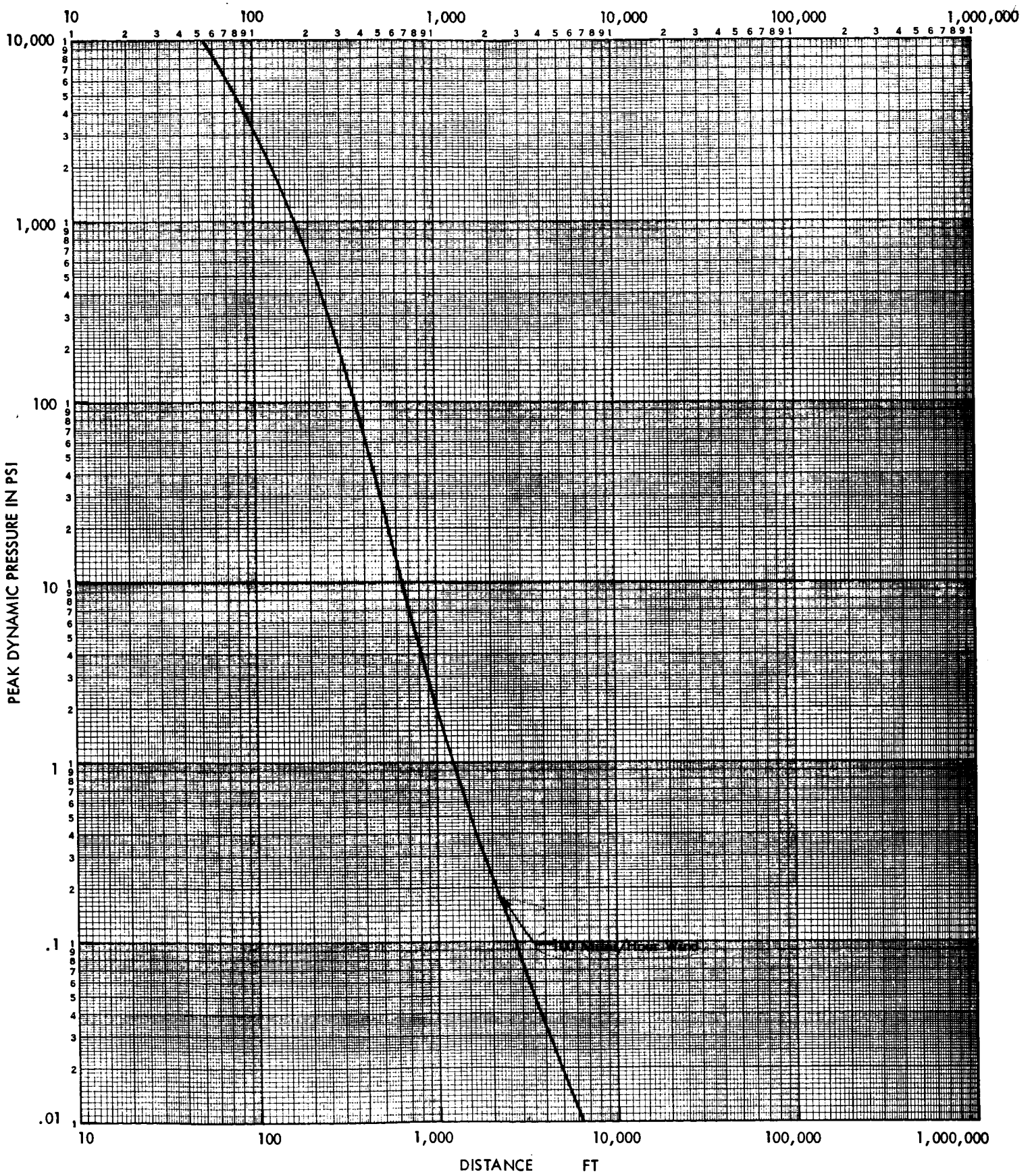

Figure 10. Peak Dynamic Pressure versus Distance for 10^6 lb T.N.T. Surface Explosion

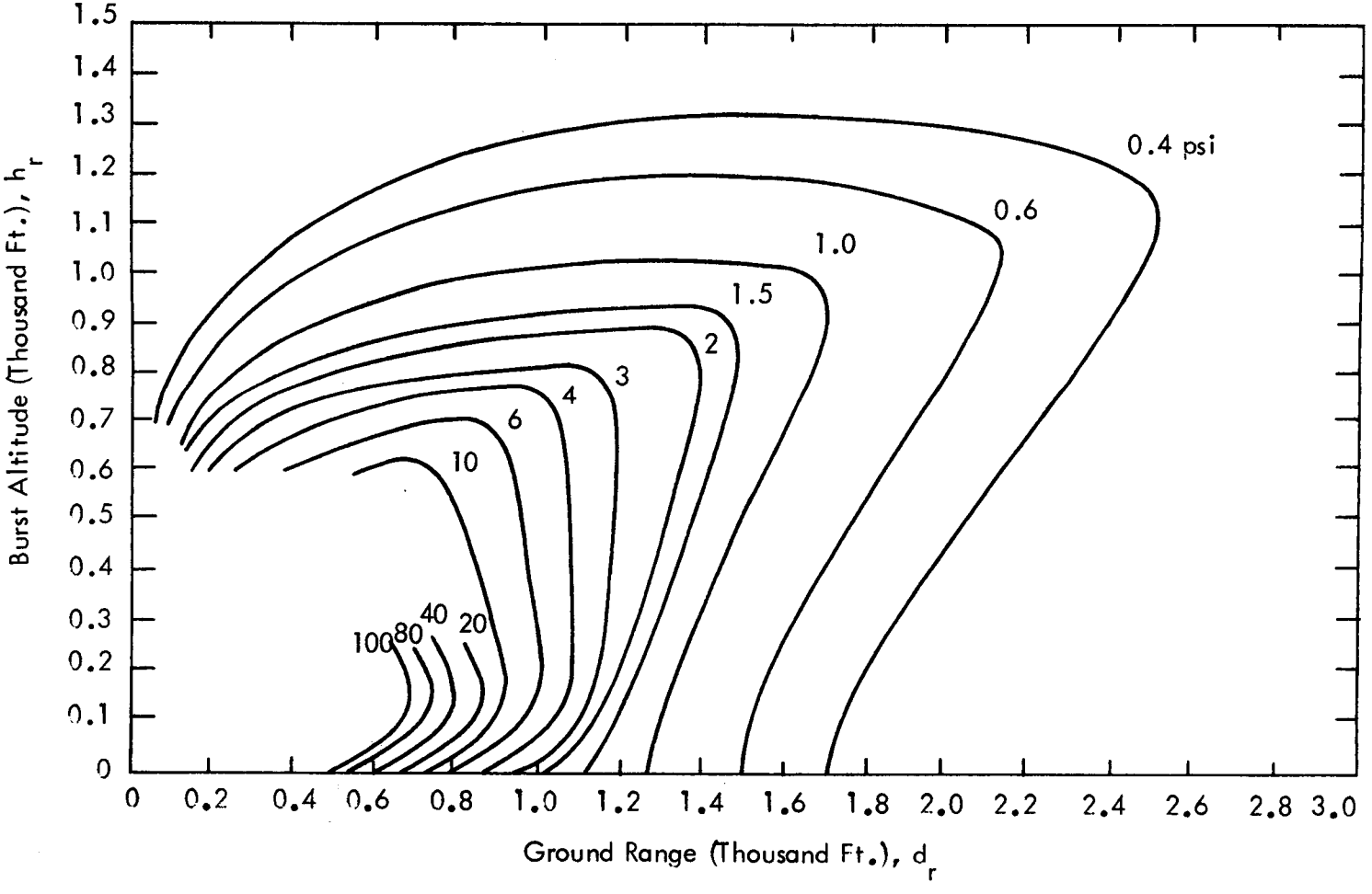

Figure 11: Peak Dynamic Pressure on the Surface (Horizontal Component) as a Function of Height of Burst and Ground Zero Distance; 10^6 lb of TNT at Sea Level for Average Surface Conditions

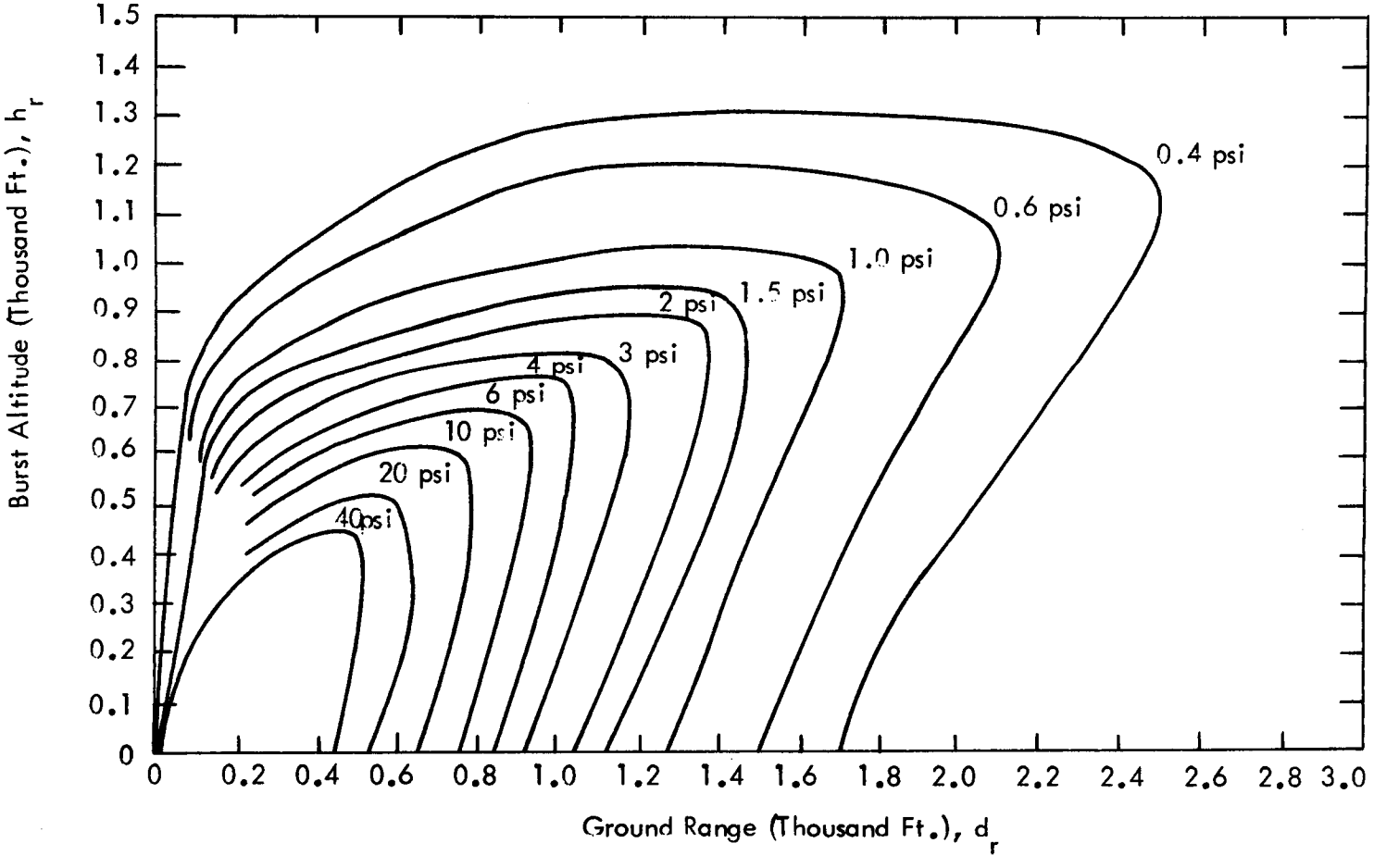

Figure 12: Peak Dynamic Pressure on the Surface (Horizontal Component) as a Function of Burst Altitude and Ground Zero Distance; 10^6 lb of TNT at Sea Level for Good Surface Conditions

Comments: When the peak dynamic pressure is $\lesssim 1.47$ psi, for inflight explosions, Figures 11 and 12 cannot be used, and Figure 10 should be used and entered merely with the ground zero reference distance (d_r). The resons for this are: the altitude effects decrease with increasing distance and the accuracy in calculations accounting for altitude effects progressively decreases with increasing distance so that beyond a certain value of peak dynamic pressure Figure 10 and Figures 11 and 12 read the same within the reliability limits. Moreover, for peak overpressures $\lesssim 1.47$ psi the dynamic pressure could be neglected as explained in Appendix D. However, the peak dynamic pressure for a peak overpressure of 1.47 psi will be calculated both as an example and as a check on its lack of significance for a case in which the highest possible accuracy is required. The relative magnitude of the dynamic pressure with respect to overpressure for overpressures $\lesssim 1.47$ psi is shown by Figure 18.

Examples:

(a) Given - A far-field-TNT-equivalency of 5×10^6 lb (WT) and assuming a ground explosion.

(a1) Find - The peak dynamic pressure (q_s) at a distance of 1,370 ft. (where $p_s = 14.7 \pm 1.47$ psi).

Solution - Define the surface conditions: To be conservative, assume good ground conditions. From Figure 10, q_s can be found knowing the reference distance, d_r. Applying the scaling laws, (Section 2.0):

$$d_r = d\,(WT_r/WT)^{1/3} = 0.80 \times 10^3 \text{ ft.}$$

and from Figure 10 $q_s = 4.0$ psi.

Considering the reliability of Figure 10, ($\pm$ 25 percent) we have:

$$q_s = (4.0 \pm 1.0) \text{ psi}$$

(a2) Find - The peak dynamic pressures (q_s) at a distance of 5,810 ft. (where $p_s = 1.47 \pm .147$ psi).

Repeating the procedure outlined in example (a1) it is found:

$$q_s = (0.052 \pm 0.010) \text{ psi}$$

Notice that a wind of 16.8 miles per hour would give a dynamic pressure of .05 psi.

(b) Given - A far-field-TNT-equivalency of 5×10^6 lb (WT).

(b1) Find - The peak dynamic pressure (q_s) at a distance of 1,740 ft. from ground zero assuming the explosion to occur at an altitude of about 1,000 ft. (the peak overpressure at the same point would be 14.7 psi).

Solution - Define the surface conditions: Assume good ground conditions. From Figure 12, q_s can be found knowing the reference distance and the reference altitude for the explosion under consideration.

Applying the scaling laws (Section 2.0):

$$d_r = d\,(WT_r/WT)^{1/3} = 1.02 \times 10^3 \text{ ft}$$

$$h_r = h\,(WT_r/WT)^{1/3} = 0.585 \times 10^3 \text{ ft.}$$

and from Figure 12, $q_s = 4.20$ psi.

Considering the reliability of Figure 12, ($\pm$ 25 percent) we might have:

$$q_s = (4.20 \pm 1.05) \text{ psi}$$

(b2) Find - The peak dynamic pressure (q_s) at a distance of 8,200 ft. from ground zero assuming the explosion to occur at an altutude of about 2,700 ft. (the peak overpressure at the same point would be 1.47 psi).

Solution - Repeating the reasoning of the preceding solution, Figure 12 gives q_s, knowing the reference distance and the reference altitude for the explosion under consideration.

Applying the scaling laws, (Section 2.0):

$$d_r = d\,(WT_r/WT)^{1/3} = 4.80 \times 10^3 \text{ ft.}$$

$$h_r = h\,(WT_r/WT)^{1/3} = 1.58 \times 10^3 \text{ ft.}$$

The point for $d_r = 4{,}800$ ft. and $h_r = 1{,}580$ ft. lies outside the limits of Figure 12 so that Figure 10 has to be used. Entering Figure 10 with $d_r = 4{,}800$ ft., we read $q_s = .021$ psi.

Considering the reliability of Figure 10 ($\pm$ 25 percent)

$$q_s = (0.021 \pm 0.005) \text{ psi}$$

4.2.3 Durations of Positive Phases: t_p^+ and t_q^+

Figures 13 and 14 can be used.

Reliability: Time durations from Figure 13 are reliable to $\pm$ 10 percent. Time variations from Figure 14 are reliable only to $\pm$ 50 percent.

Comments: Reliability of the time duration of positive phases are low essentially because such durations are sensitive to several physical parameters, (See Appendix D).

Examples:

(a) Given - A far-field-TNT-equivalency of 5×10^6 lb TNT (WT) and assuming ground explosion.

(a1) Find - The duration of positive overpressure phase (t_p^+) and of positive dynamic pressure phase (t_q^+) at a distance of 1,370 ft. (where the peak overpressure would be 14.7 ± 1.47 psi)

Solution - From Figure 13, the two durations (t_p^+ and t_q^+) can be estimated knowing the reference distance for the explosion under consideration.

Applying the scaling laws, (Section 2.0):

$$d_r = d\,(WT_r/WT)^{1/3} = 0.80 \times 10^3 \text{ ft.}$$

and from Figure 13 $(t_p^+)_r = 0.31$ sec. and $(t_q^+)_r = 0.375$ sec.

Applying again the scaling laws:

$$t_p^+ = (t_p^+)_r\,(WT/WT_r)^{1/3} = 0.530 \text{ sec.}$$

$$t_q^+ = (t_q^+)_r\,(WT/WT_r)^{1/3} = 0.642 \text{ sec.}$$

Considering the reliability of Figure 13 ($\pm$ 10 percent), we have:

$$t_p^+ = (0.530 \pm 0.053) \text{ sec.}$$

$$t_q^+ = (0.642 \pm 0.064) \text{ sec.}$$

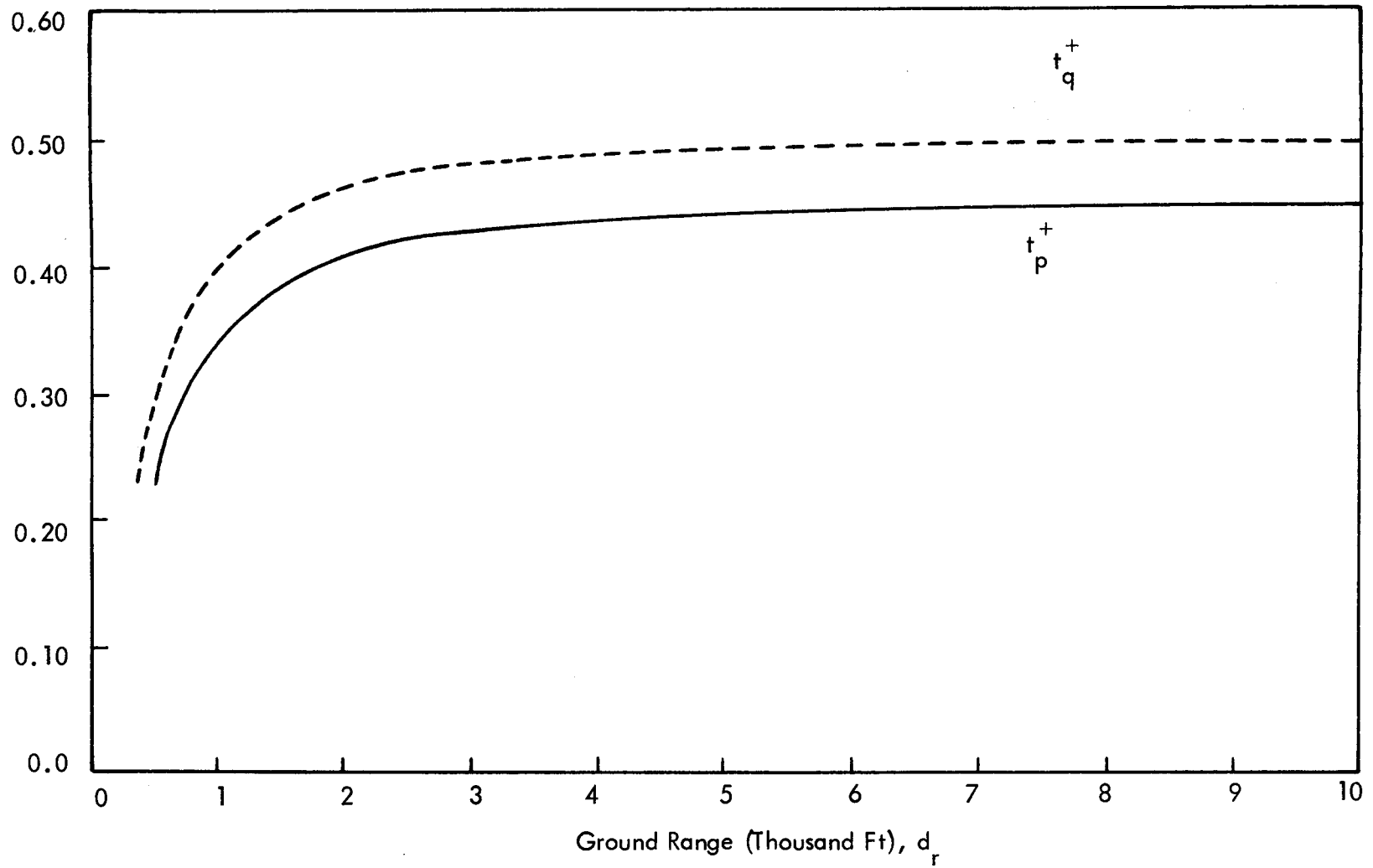

Figure 13: Durations of Positive Phases of Overpressure and Dynamic Pressure versus Distance for a 10^6 lb Far-Field-TNT-Equivalent Rocket Explosion on the Ground

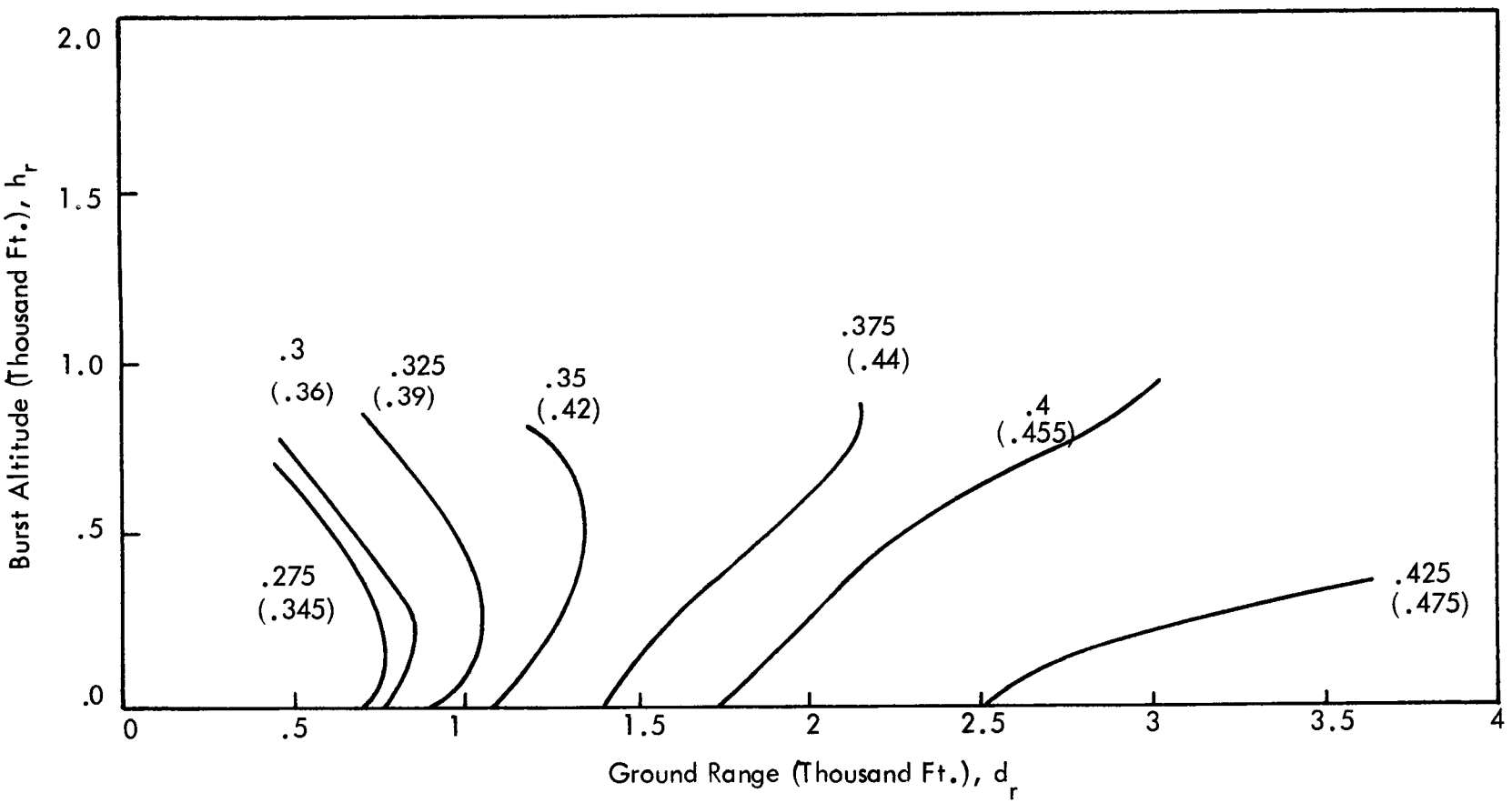

Figure 14: Durations of Positive Phases of Overpressure and Dynamic Pressure (in parentheses) versus Burst Altitude and Ground Zero Distance for a 10^6 lb Far-Field-TNT-Equivalent Rocket Explosion

(a2) Find - The duration of positive overpressure phase (t_p^+) and of positive dynamic pressure phase (t_q^+) at a distance of 5,810 ft. (where the peak overpressure would be 1.47 $\pm$ 0.147 psi).

Repeating the procedure outlined in example (a1) it is found:

$$t_p^+ = (0.786 \pm 0.079) \text{ sec.}$$

$$t_q^+ = (0.839 \pm 0.084) \text{ sec.}$$

(b) Given - A far-field-TNT-equivalency of 5×10^6 lb.

(b1) Find - The durations of positive overpressure phase (t_p^+) and of positive dynamic pressure phase (t_q^+) at a distance of 1,745 ft. from ground zero assuming the explosion to occur at an altitude of about 1,000 ft. (the overpressure at the same point would be 14.7 $\pm$ 2.94 psi).

Solution - From Figure 14 the two durations (t_p^+) and (t_q^+) can be estimated knowing the reference altitude and reference distance for the explosion under consideration.

Applying the scaling laws, (Section 2.0):

$$d_r = d\ (WT_r/WT)^{1/3} = 1.020 \times 10^3 \text{ ft.}$$

$$h_r = h\ (WT_r/WT)^{1/3} = 0.585 \times 10^3 \text{ ft.}$$

and from Figure 14 we read $(t_p^+)_r = 0.33$ sec. and $(t_q^+)_r = 0.397$ sec.

Applying again the scaling laws:

$$t_p^+ = (t_p^+)_r\ (WT/WT_r)^{1/3} = 0.564 \text{ sec.}$$

$$t_q^+ = (t_q^+)_r\ (WT/WT_r)^{1/3} = 0.678 \text{ sec.}$$

Considering the reliability of Figure 14 ($\pm$ 50 percent) we have:

$$t_p^+ = (0.564 \pm 0.282) \text{ sec.} \quad \text{and} \quad t_q^+ = (0.678 \pm 0.339) \text{ sec.}$$

(b2) Find - The durations of positive overpressure phase (t_p^+) and of positive dynamic pressure phase (t_q^+) at a distance of 8,200 ft. from ground zero assuming the explosion to occur at an altitude of about 2,700 ft. (The overpressure at the same point would be 1.47 $\pm$ 0.294 psi).

Solution - From Figure 14, the two durations (t_p^+ and t_q^+) can be estimated knowing the reference altitude and reference distance for the explosion under consideration.

Applying the scaling laws, (Section 2.0):

$$d_r = d\ (WT_r/WT)^{1/3} = 4.80 \times 10^3 \text{ ft.}$$

$$h_r = h\ (WT_r/WT)^{1/3} = 1.58 \times 10^3 \text{ ft.}$$

Since d_r and h_r are out of the range of Figure 14, Figure 13 has to be used. From Figure 13, with d_r = 4,800 ft., we read $(t_p^+)_r$ = 0.445 sec. and (t_q^+) = 0.490 sec.

Applying again the scaling laws:

$$t_p^+ = (t_p^+)_r\ (WT/WT_r)^{1/3} = 0.760 \text{ sec.}$$

$$t_q^+ = (t_q^+)_r\ (WT/WT_r)^{1/3} = 0.838 \text{ sec.}$$

Considering the reliability of Figure 13 ($\pm$ 10 percent) we have:

$$t_p^+ = (0.760 \pm 0.076) \text{ sec.}$$

$$t_q^+ = (0.838 \pm 0.084) \text{ sec.}$$

4.2.4 Time Variations of Overpressure and Dynamic Pressure

Figures 15 and 16 can be used.

Reliabilities and Comments: Figures 15 and 16, from reference 3 - 1955 may be used to define two ranges of time variations of overpressure and dynamic pressure by the previously calculated peak overpressure and overpressure durations and peak dynamic pressure and dynamic pressure duration with their relative reliability limits. All the curves within the above defined ranges have to be considered possible; hence, the worst of them, from a structural design viewpoint, should be considered. The average curve is the most probable one.

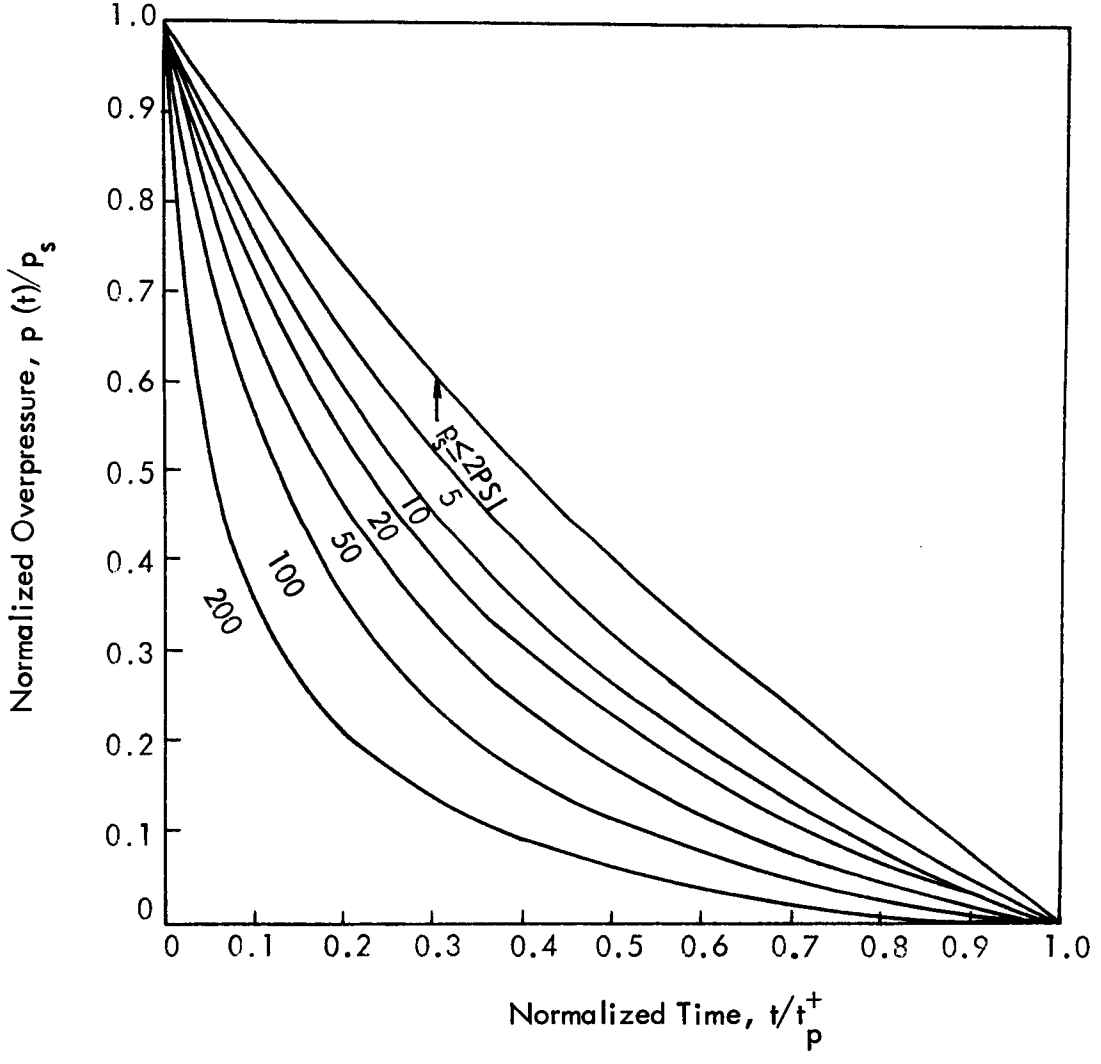

Figure 15: Rate of Decay of Pressure with Time for Various Values of the Peak Overpressure.

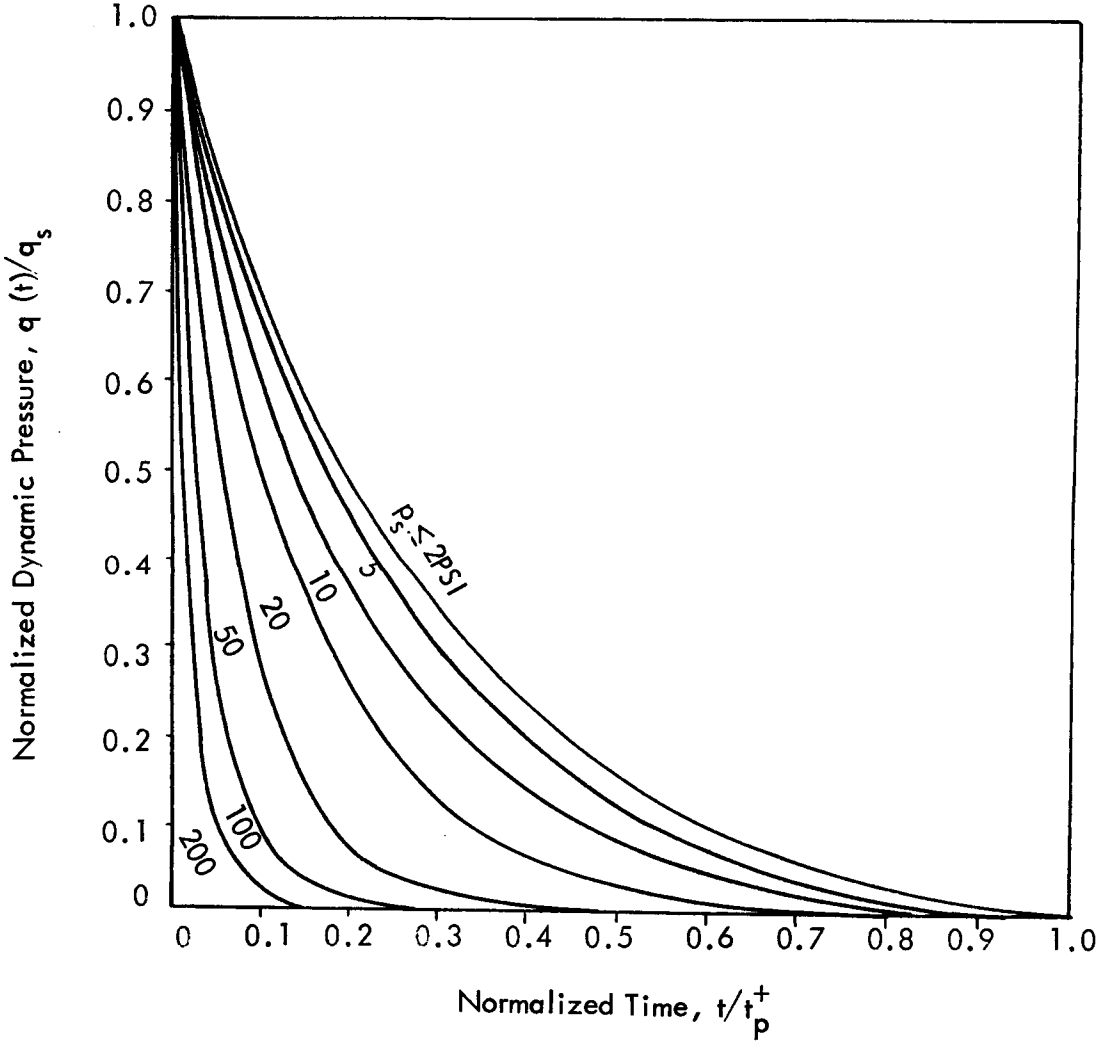

Figure 16: Rate of Decay of Dynamic Pressure with Time for Various Values of the Peak Overpressure.

Examples:

(a) Given - A far-field-TNT-equivalency of 5×10^6 lb (WT) and assuming a ground explosion.

(a1) Find - The time variations of overpressure and dynamic pressure at a distance of 1,370 ft. (where $p_s = 14.7 \pm 1.47$ psi).

Solution - It is necessary to have already determined peak dynamic pressures and overpressure and dynamic pressure positive phase durations with their relative reliability limits. This was accomplished in examples (a1) of Sections 4.2.2, and 4.2.3. The results were:

Peak overpressure: $p_s = 14.7 \pm 1.47$ psi

Peak dynamic pressure: $q_s = 4.0 \pm 1.0$ psi

Overpressure positive phase duration: $t_p^+ = 0.530 \pm 0.053$ sec.

Dynamic pressure positive phase duration: $t_q^+ = 0.642 \pm 0.064$ sec.

Now we can use Figures 15 and 16 to calculate the following tables.

From Figure 15:

Read From Figure 15		Calculate from First Two Columns by Setting: $p_s = 16.17$ psi, $t_p^+ = 0.583$ sec.		Calculate From First Two Columns by Setting: $p_s = 13.23$ psi, $t_p^+ = 0.477$ sec.	
$p(t)/p_s$	t/t_p^+	$p(t)$	t	$p(t)$	t
1.0	0.0	16.17	0.0	13.23	0.0
0.9	0.040	14.55	0.023	11.90	0.019
0.8	0.075	12.90	0.044	10.60	0.037
0.7	0.120	11.30	0.070	9.25	0.057
0.6	0.175	9.70	0.102	7.93	0.083
0.5	0.245	8.09	0.143	6.61	0.117
0.4	0.320	6.46	0.186	5.30	0.153
0.3	0.430	4.85	0.250	3.97	0.205
0.2	0.570	3.24	0.332	2.64	0.272
0.1	0.740	1.617	0.431	1.32	0.353
0.0	1.0	0.0	0.583	0.0	0.470

And from Figure 16:

Read From Figure 16		Calculated from First Two Columns by Setting: $q_s = 5.0$ psi $t_q^+ = 0.706$ sec.		Calculated from First Two Columns by Setting: $q_s = 3.0$ psi $t_q^+ = 0.578$ sec.	
$q(t)/q_s$	t/t_q^+	$q(t)$	t	$q(t)$	t
1.0	0.0	5.00	0.0	3.00	0.0
0.9	0.020	4.50	0.014	2.70	0.011
0.8	0.035	4.00	0.025	2.40	0.020
0.7	0.060	3.50	0.042	2.10	0.035
0.6	0.085	3.00	0.060	1.80	0.049
0.5	0.115	2.50	0.081	1.50	0.066
0.4	0.160	2.00	0.113	1.20	0.092
0.3	0.210	1.50	0.148	0.90	0.121
0.2	0.280	1.00	0.198	0.60	0.162
0.1	0.400	0.50	0.282	0.30	0.231
0.0	1.0	0	0.706	0.0	0.578

The results of the above two tables are plotted on Figure 17.

Any curve within the calculated range is acceptable, the average curve being the more likely one.

(a2) Find - The time variation of overpressure and dynamic pressure at a distance of 5,810 ft., (where $p_s = 1.47 \pm .147$ psi).

Solution - It is necessary to have already determined peak dynamic pressure and overpressure and dynamic pressure positive phase durations with their relative reliability limits. This was accomplished in instances (a2) of Sections 4.2.2, and 4.2.3. The results being:

Peak overpressure: $p_s = 1.47 \pm .147$ psi

Peak dynamic pressure: $q_s = 0.052 \pm 0.010$ psi

Overpressure positive phase duration: $t_p^+ = 0.786 \pm 0.079$ sec.

Dynamic pressure positive phase duration: $t_q^+ = 0.839 \pm 0.084$ sec.

Now we can use Figures 15 and 16 to calculate the following tables:

From Figure 15

Read From Figure 15		Calculated from First Two Columns by Setting: $p_s = 1.617$ psi $t_p^+ = 0.865$ sec.		Calculated from First Two Columns by Setting: $p_s = 1.323$ psi $t_p^+ = 0.707$ sec.	
$p(t)/p_s$	t/t_p^+	$p(t)$	t	$p(t)$	t
1.0	0.0	1.617	0.0	1.323	0.0
0.9	0.07	1.455	0.060	1.190	0.045
0.8	0.15	1.295	0.130	1.060	0.108
0.7	0.23	1.132	0.199	0.926	0.162
0.6	0.31	0.970	0.268	0.794	0.219
0.5	0.40	0.809	0.346	0.661	0.283
0.4	0.50	0.647	0.432	0.530	0.354
0.3	0.62	0.485	0.536	0.397	0.439
0.2	0.75	0.323	0.650	0.265	0.530
0.1	0.87	0.162	0.753	0.132	0.615
0.0	1.0	0.0	0.865	0.0	0.707

And from Figure 16

Read From Figure 16		Calculated from First Two Columns by Setting: $q_s = 0.062$ psi $t_q^+ = 0.923$ sec.		Calculated from First Two Columns by Setting: $q_s = .042$ psi $t_q^+ = .755$ sec.	
$q(t)/q_s$	t/t_p^+	$q(t)$	t	$q(t)$	t
1.0	0.0	0.062	0.0	0.042	0.0
0.9	0.03	0.056	0.028	0.037	0.022
0.8	0.07	0.050	0.065	0.033	0.053
0.7	0.10	0.043	0.092	0.029	0.075
0.6	0.14	0.037	0.134	0.025	0.109
0.5	0.20	0.031	0.184	0.021	0.151
0.4	0.26	0.025	0.240	0.016	0.196
0.3	0.34	0.019	0.314	0.012	0.256
0.2	0.44	0.012	0.406	0.083	0.332
0.1	0.59	0.062	0.545	0.042	0.445
0.0	1.0	0.0	0.923	0.0	0.755

The results of the above two tables are plotted on Figure 18.

Any curve within the calculated range is acceptable, the average curve being the more likely one.

For the sake of uniformity, we should now calculate the time variations of overpressure and dynamic pressure for the worst inflight explosion at ground zero distances of 1,745 and 8,200 ft. to where the overpressure would be 14.7 ± 1.47 and 1.47 ± 0.147 psi, respectively. Data from example (b1) of Sections 4.2.2, and 4.2.3 can be used to calculate the time variations for an overpressure of 14.7 psi, and data from examples (b2) of Sections 4.2.2, and 4.2.3 to calculate the time variations for an overpressure of 1.47 psi, for the worst inflight explosion. However, since the procedure would be exactly equal to that followed in examples (a1) and (a2) of the present section, further repetition is not considered useful. The results of the examples of Section 4.0 are summarized in Table III.

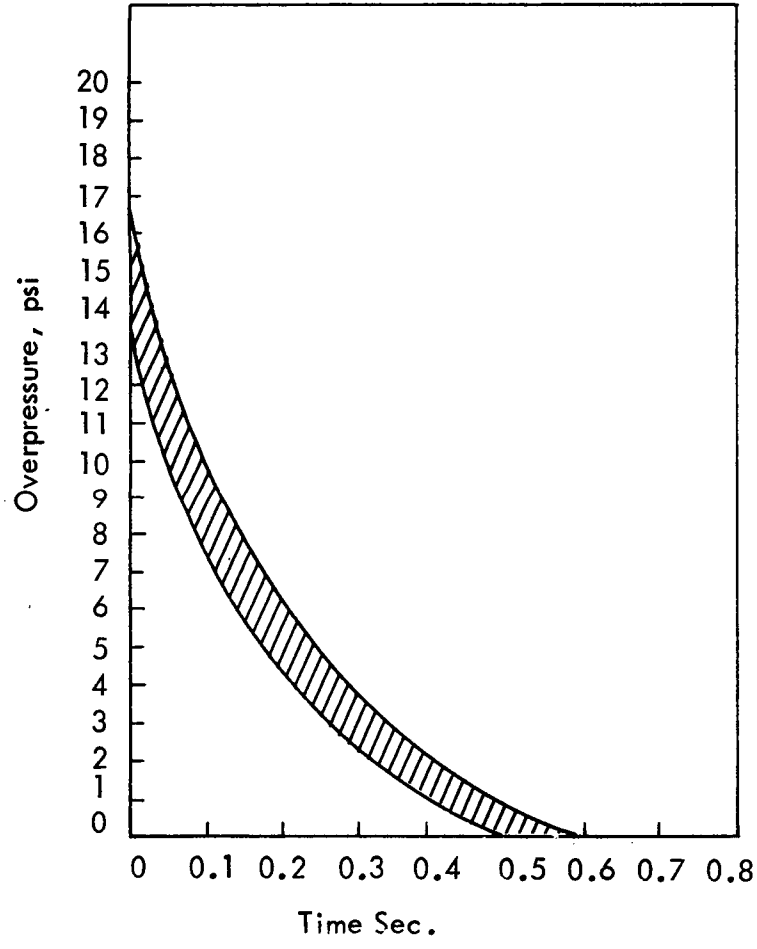

Figure 17: Time Variation of Overpressure at a Distance of 1,370 ft. from a 10^6 lb Far-Field-TNT-Equivalent Rocket Explosion

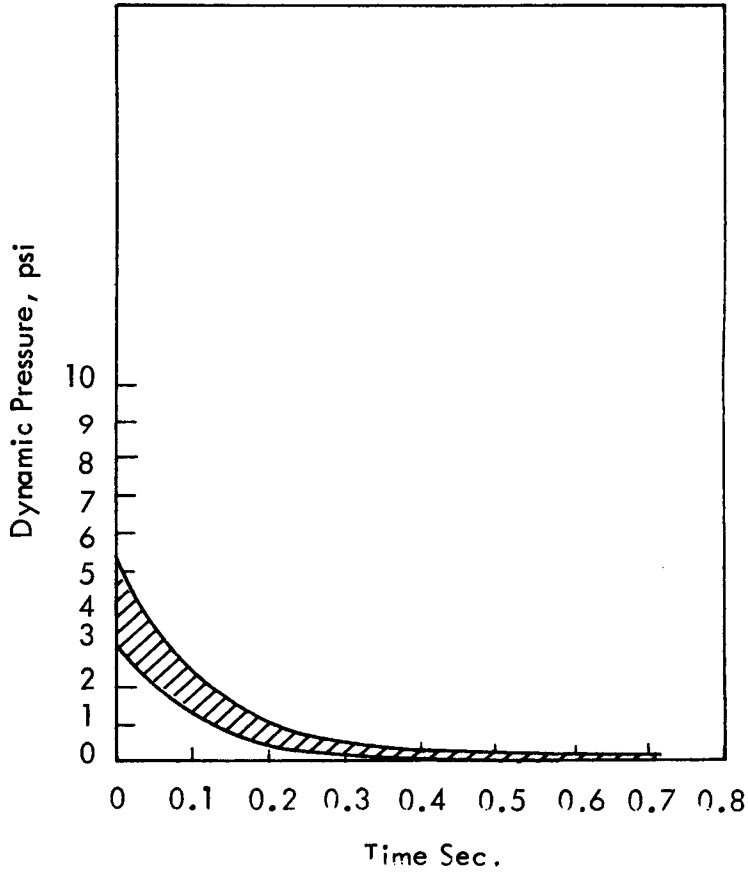

Time Variation of Dynamic Pressure at a Distance of 1,370 ft. from a 10^6 lb Far-Field-TNT-Equivalent Rocket Explosion

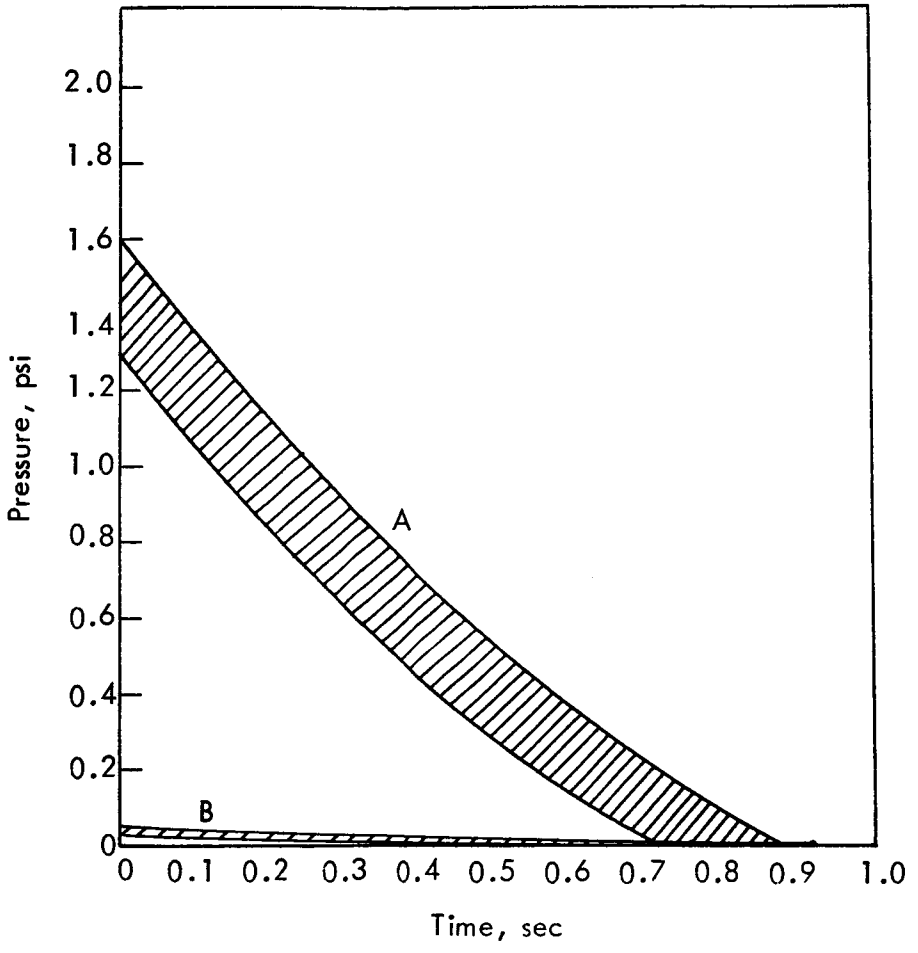

Figure 18: A: Time Variation of Overpressure at a Distance of 5,810 feet from a 10^6 lb Far-Field-TNT-Equivalent Rocket Explosion

B: Time Variation of Dynamic Pressure at a Distance of 5,810 feet from a 10^6 lb Far-Field-TNT-Equivalent Rocket Explosion

TABLE III

SUMMARY OF THE AIR SHOCK PARAMETERS FROM A 5×10^6 Lb. FAR-FIELD-TNT-EQUIVALENT ROCKET EXPLOSION AT PEAK OVERPRESSURES OF 0.0147, 1.47, AND 14.7 psi

Parameters	For p_s=0.0147 psi		For p_s= 1.47 psi		For p_s= 14.7 psi	
	Values	Section	Values	Section	Values	Section
Distance (thousand of feet)	Slant Distances		Ground Distances		Ground Distances	
	240 ± 40.8		5.810+ 0.581		1.370+ 0.137	
Distance (thousand of feet) for worst inflight explosion	240± 40.8	4.1.1	8.20+ 1.39	4.2.1	1.74+ 0.296	4.2.1
Altitude (thousand of feet) for worst inflight explosion	——	4.1.1	1.98 to 3.60	4.2.1	0.71 to 1.32	4.2.1
Peak dynamic pressure (psi) for ground explosion (q_s)	Negli-		0.052±		4.0 ±	
	gible	4.1.2	0.010	4.2.2	1.0	4.2.2
Peak dynamic pressure (psi) for worst inflight explosion (q_s)	Negli- gible		0.021 ± 0.005		4.2± 1.05	
Overpressure positive phase duration (sec.) for ground explosion (t_p^+)	0.780± 0.078		0.786 ± 0.079		0.530± 0.053	
Dynamic pressure positive phase duration (sec.) for ground explosion (t_q^+)	——	4.1.3	0.839 ± 0.084	4.2.3	0.642± 0.064	4.2.3
Overpressure positive phase duration (sec.) for worst inflight explosion (t_p^+)	0.780± 0.078		0.760± 0.076		0.564± 0.282	
Dynamic pressure positive phase duration (sec.) for worst inflight explosion (t_p^+)	——		0.838 ± 0.084		0.678± 0.339	
Pressure time variation for ground explosion	See Sec.3.4					
Dynamic pressure time variation for ground explosion	Negli- gible					
Pressure time variation for worst inflight explosion	See Sec.3.4	4.1.4	See Fig. 18	4.2.4	See Fig. 17	4.2.4
Dynamic pressure time variation for worst inflight explosion	Negli- gible					

5.0 CONCLUSIONS

Three ranges in the blast field from LH_2 - LO_2 and RP-1-LO_2 propellant explosions were defined in terms of peak overpressure; namely, the close -, medium- and far-fields. For the medium- and far-fields and for large rocket explosions, the TNT equivalency system was found acceptable to estimate the air shock parameters. For the close-field the TNT equivalency system was shown to lead to over conservative estimates. Accordingly, charts and recommendations for the air blast parameters in the medium- and far-fields, based on the TNT equivalency system, were presented. Future work to compute the close-field air blast parameters was outlined. Several aspects of the explosion phenomenon, such as the origin of the air blast, the influence of the physical and chemical properties of the explosive, the scaling laws, and the air blast equations were also discussed with the conclusion that more individual computations should be made for each of the propellants considered. Finally, a general conclusion was made that improved close-field estimates for rocket explosions would be of significant economical importance to the agencies and industries which deal with liquid propellant explosion hazards.

APPENDIX A

UNCONTROLLED CHEMICAL REACTION; RATE OF ENERGY RELEASE; DEFLAGRATION AND DETONATION

For an explosion to occur, the propellants must first of all mix accidentally. This can occur, for instance, because of leaks or ruptures of the tanks or propellant feed systems. The fuel to oxidizer mixture ratio must fall within a certain range before the reaction can start. This reaction can then start spontaneously because of the strong affinity of the propellants hypergolic propellants) or be started by external energy sources such as: heat, an electrical spark, shock, friction, etc. Once the reaction is started, the heat released by the initial reaction will be sufficient to trigger further reaction in the remaining propellants. The speed of this chain reaction defines the rate of energy release for given propellants. The rate of energy release is not a constant but varies with the mixture ratio, the temperature of the propellants, the degree of turbulence, and the amount of propellant.

When the chemical reaction process occurs at a low rate of energy release, it is called a (slow) burning or deflagration. In both cases, the effects are: the speed of the flame front is subsonic, the burned gas flows away from the flame front, and the pressure drops through the flame front. But the magnitudes of these effects are different. If the reaction process occurs at a high rate of energy release, the reaction is called a detonation and it is characterized by a reaction front moving at a supersonic speed, burned gas flowing after the front, and a pressure increase through the front (now called a shock front). A detonation wave in the propellants generates the shock wave in air that characterizes the blast from rocket explosions. Thus, the capability of some propellants to react at a high rate of energy release makes them possible "explosives". The high rate of energy release also defines the difference between a common explosive (TNT) and ordinary fuels. The explosion energy per unit weight of the most energy rich explosives does not exceed that of normal fuels as the first column of the following table shows. Yet a conventional explosive releases its energy in a much shorter time giving a higher volume concentration of energy for its products of reaction as the second column of the following table shows:

TABLE IV

EXPLOSION ENERGY PER UNIT WEIGHT OF SOME EXPLOSIVES AND FUEL MIXTURES AND ENERGY PER UNIT VOLUME OF THEIR RESPECTIVE PRODUCTS OF REACTION

Explosive or Fuel	Explosion Energy Per Unit Weight (Kcal/Kg)	Energy Per Unit Volume of the Products (Kcal/l)
Pyroxylin (13.3 percent N)	1040	1350
Nitroglycerine	1485	2380
Mixture of Benzene and Oxygen	2330	4.1
Mixture of Carbon and Oxygen	2130	4.4
Mixture of Hydrogen and Oxygen	3230	1.7

(From Reference 7).

From the given data it is seen that during the explosion of a standard explosive, the energy within a given volume is hundreds of times the energy within the same volume during the explosion of standard fuels. Experiments show (see 2.0 and 1.4), that for RP-1-LO_2, for instance, the far-field TNT equivalent for small explosions is about 10 percent. Consider one pound of TNT and ten pounds of RP-1-LO_2; far from the explosion site the energies released by the two explosions would be equal. Isolate a volume within the TNT charge and the same volume within the RP-1-LO_2 charge. When in the two charges the detonation shocks have reached the volume surfaces, the energies within the two volumes are different. The energy in the TNT volume is hundreds of times the energy in the RP-1-LO_2 volume, yet in the far-field the two energies will be equal. There is only one explanation: energy is released by the RP-1-LO_2 charge during a longer time. During all this time the energy actually available to the air shock from the RP-1-LO_2 charge is lower than for the TNT charge. With this time there is associated a certain distance that the air shock has traveled, and with this distance, a region around the explosion site. This region is the close-field and within this region the air shock from LO_2-RP-1 explosion will be weaker than the air shock from a TNT explosion of far-field equal energy. In closing this Appendix, it might be useful to notice that an extensive study of most of the explosion problems can be found in Reference 7. Reference 7 can be used, for example, for the determination of the theoretical explosive energies of propellants which have not been considered in this report.

APPENDIX B

THE ORIGIN OF THE AIR BLAST; BOUNDARY PROBLEM AT THE INTERFACE BETWEEN PROPELLANT MIXTURE AND AIR; INITIAL AIR SHOCK VELOCITY

As pointed out by Rudlin in Reference 9, there is some disagreement between present theoretical predictions and experimental measurements of initial air blast velocity.

When the detonation shock moving through the explosive gets to the interface between the explosive and air, a shock is originated in air and a new perturbation (expansion wave) moves back from the interface toward the center of the explosion. From present state-of-the-art theory, one calculates two different velocities for the shock in the explosive and in air primarily because of the difference in impedance (the product of the unperturbed density and shock velocity) of the two media.

Experimental results tend to show that such a difference does not exist, (references 9 and 10). Figure 19 shows no discernable change in the slope of the distance - time curve describing the motion of the shock from a gaseous mixture into air. Figure 20 shows the same trend for the motion of the shock from a solid charge into air. These data are considered to be sufficient to justify the assumption that the initial air shock velocity is equal to the detonation velocity of the exploding material when estimates for the close-field air shock parameters are of interest.

At least one explanation for the disagreement between theory and the experimental data is that the currently applied theory does not take into account the chemical reaction in the explosion products, thus, treating the problem as that of the transmission of a shock through an interface between chemically stable media.

In this present theory, (see Reference 12), the shock equations are applied to the two media and particular conditions imposed at the interface. For the shock moving through the explosive immediately before reaching the interface between explosive and air, the following equations can be written:

$$\rho_0' \, U' = \rho' \, (U' - u') \qquad \text{mass conservation}$$

$$p' - p_0' = \rho_0' \, u' \, U' \qquad \text{momentum conservation}$$

$$U' = u' + c' \qquad \text{Chapman - Jouguet condition}$$

$$c' = (\gamma \, p'/\rho')^{1/2}$$

For the shock moving through air after passing the explosive-air interface:

$$\rho_0 \, U = \rho \, (U - u) \qquad \text{mass conservation}$$

$$p - p_0 = \rho_0 \, u \, U \qquad \text{momentum conservation}$$

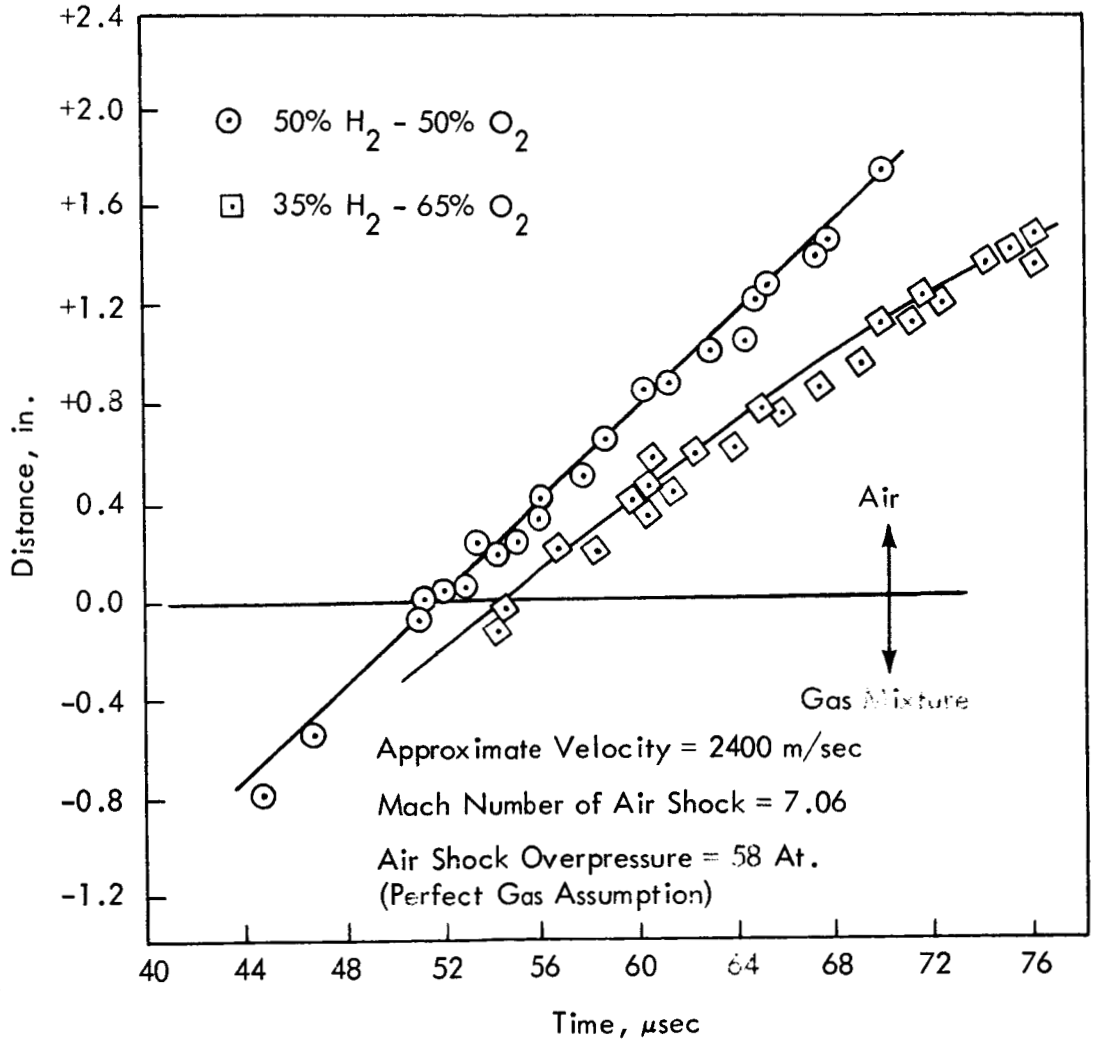

Figure 19. Distance of Wave-Front from Tube Exit Versus Time Delay for Hydrogen-Oxygen Mixtures Next to an Air Boundary. (From Reference 10)

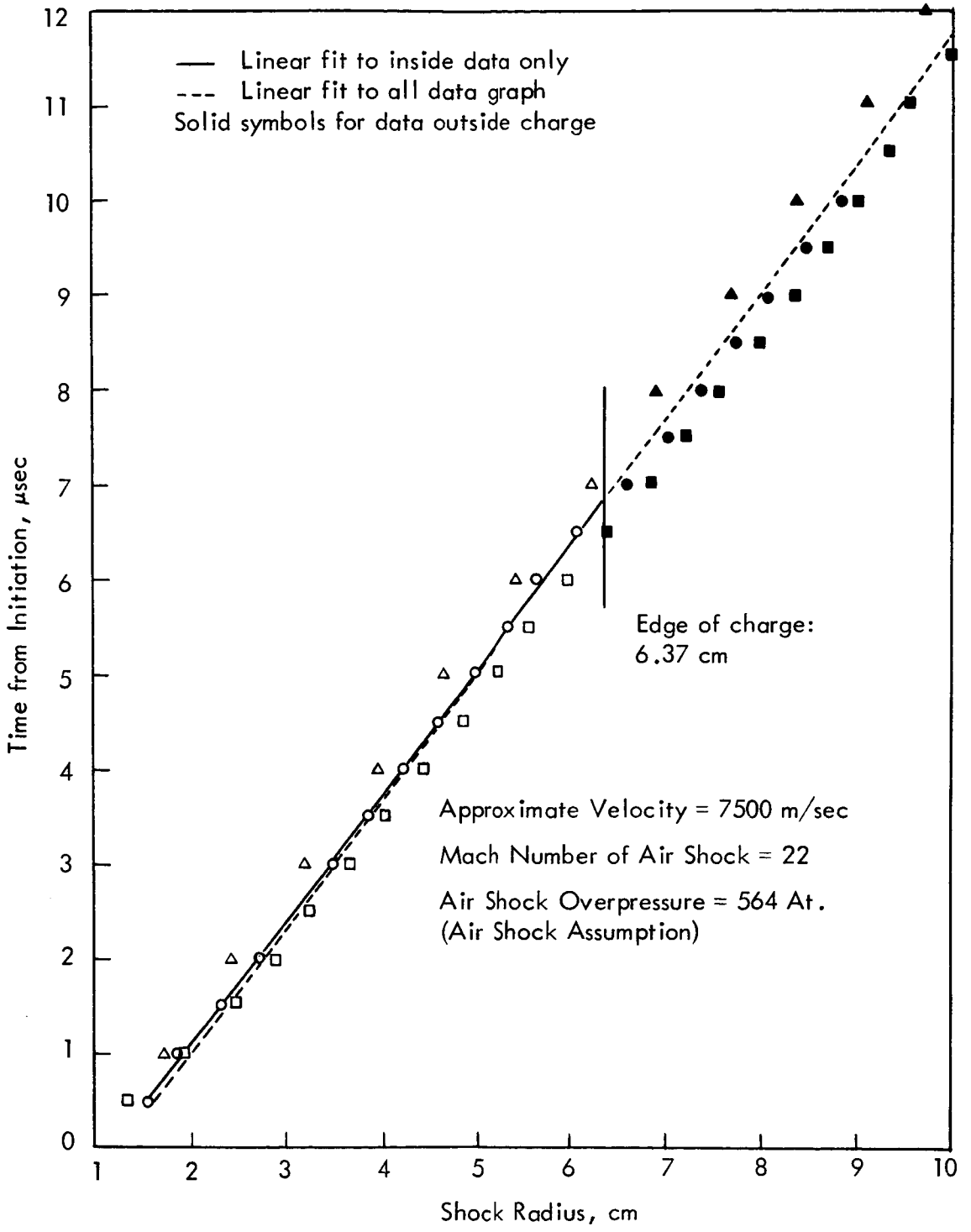

Figure 20. Time Versus Shock Radius for Cast Pentolite (From Reference 9)

It is then assumed that at the interface a expansion wave moving toward the center is generated and for this wave, the particle velocity of the explosion gases expanded from ρ' to ρ'' is given by:

$$u'' = u' + \int_{\rho'}^{\rho''} c \, \frac{d\rho'}{\rho'}$$

and, furthermore, it is assumed that $u'' = u$ and $p'' = p$ while $p'_0 = p_0 = 0$. The system of equations is then sufficient to determine the variables once that state equations or further process assumptions are also used. When no chemical reaction is present and the medium through which the first shock passed is polytropic, the solution reached above gives satisfactory results as in the case of propagation of a shock from water to air. But in the case of an explosion, the above set of equations and of assumptions is at least oversimplified.

A better set would be through the shock in the explosive:

$$\rho'_0 \, U' = \rho' \, (U' - u')$$

$$p' - p'_0 = \rho'_0 \, u' \, U'$$

$$U' = u' + c'$$

$$c' = (\gamma \, p'/\rho')^{1/2}$$

$$E - H = \frac{1}{2} \, (p' - p'_0) \, \left(\frac{1}{\rho'_0} - \frac{1}{\rho'}\right)$$

where E = internal energy of the exploded material; H = chemical energy released

Through the shock in air:

$$\rho_0 \, U = \rho \, (U - u)$$

$$p - p_0 = \rho_0 \, u \, U$$

$$e - e_0 = \frac{1}{2} \, (p - p_0) \, \left(\frac{1}{\rho_0} - \frac{1}{\rho}\right)$$

where e = internal energy of the air.

The expansion wave equation would have to be modified to include internal energy changes due to chemical reaction. The assumption to be used would be:

$$U' = U; \quad \rho_0 = \rho'_0 = 0, \quad u'' = u, \text{ and } p'' = p;$$

also, state equations and chemical equilibrium equations would need to be specified.

Such a system of equations defines the rarefaction wave, the shock within the gas of the explosion, the shock in air, and the total energy released. On the other hand the assumption $U' = U$ (initial air shock velocity equal to detonation velocity) with an estimate for the total energy released would be sufficient to provide a basis for approximate calculations of the close-field air shock parameters from rocket explosions. This approximation will be much better than the one reached through a TNT equivalency assumption, (see Reference 13). It is, in fact, the basis for the estimated close-field overpressures for rocket explosions which was shown on Figure 3.

APPENDIX C

THE SOLUTION OF THE AIR BLAST EQUATIONS AND DERIVATION OF BLAST SCALING LAWS

Air Blast Equations

For the sake of clarity a list of the symbols used in the following section is presented here:

a,b,c	=	constants
e	=	internal energy per unit of mass
$f(\ )$	=	function of $(\ )$
k	=	heat transfer coefficient
ℓ	=	Lagrangian mass coordinate
p	=	pressure
Q	=	heat added to the unit of mass
r	=	radius
s	=	entropy of the unit of mass
t	=	time
u	=	particle velocity
U	=	shock front velocity
v	=	specific volume
Δ	=	infinitesimal increment
μ	=	viscosity coefficient
ν	=	μ/ρ: Kinematic viscosity
ρ	=	density

In the following section, letter subscripts represent partial derivatives with respect to the subscript variable while number subscripts represent locations in the flow (for instance u_t = partial derivative of u with respect to t while u_1 = value of u at location 1). In particular, subscript 0 refers to conditions in front of a shock.

An air blast in uniform atmosphere is a three-dimensional flow with spherical symmetry. The conservation of mass, momentum, and energy in polar coordinates for a three-dimensional flow with spherical symmetry can be written:

1. $\rho_t + u\rho_r = -(\rho/r^2) \cdot (r^2 u)_r = -\rho (u_r + 2u/r)$

2. $u_t + uu_r = -(1/\rho)\, p_r + (1/r^2\rho) \cdot (r^2 \mu u_r)_r$

3. $e_t + ue_r = -(p/r\rho)\,(r^2 u)_r + \nu\,(u_r)^2 + (1/r^2\rho) \cdot (k r^2 T_r)_r + Q\,(r;t)$

where the independent variables are r and t and the dependent ones are ρ, u, p, e and T. Therefore, two more equations are needed. The fourth equation will be provided by the characteristics of the matter which flows (equation of state) and the fifth equation by the manner in which the flow happens (process equations). In this case the five dependent variables can be called the blast parameters and equations 1, 2, and 3 the blast equations.

Before going to the equation of state and to the process equation, the above three conservation equations will be written in forms better suited to blast propagation problems.

Equations 1, 2 and 3 for inviscid adiabatic flow become:

$$\rho_t + u\rho_r = -(\rho/r^2)\,(r^2 u)_r$$

4. $u_t + uu_r = -(1/\rho)p_r$ — Euler ref. system, 3-dimensional, inviscid, adiabatic flow with spherical symmetry. (Taylor 1941).

$$e_t + ue_r = -(p/r^2\rho)\,(r^2 u)_r = (p/\rho^2)\,(\rho_t + u\rho_r) = -p\,(v_t + uv_r)$$

The corresponding equations for one-dimensional flow are

$$\rho_t + u\rho_r = -\rho u_r$$

5. $u_t + uu_r = -(1/\rho)\, p_r$ — Euler ref. system, 1-dimensional, inviscid, adiabatic flow.

$$e_t + ue_r = -(p/\rho)\,u_r = (p/\rho^2)\,(\rho_t + up_r) = -p\,(v_t + uv_r)$$

The above equations are Euler equations of conservation of mass, momentum and energy referred to a fixed observer.

In the study of the blast propagation problem, Lagrangian equations are also used. The equations of fluid dynamics in Lagrangian form describe the motion of each element of mass (particle) as seen by an observer moving with it, using initial values of selected independent variables (Lagrangian coordinates) and time. Accordingly equations 4 and 5 are first modified for an observer moving with the particle. Then the selected independent variables are defined and mass, momentum and energy equations written in their terms. Referring to an observer

moving with the particle the convective terms (terms multiplied by u) are equal to zero. An observer moving with the particle is aware of all the flow properties and their derivatives but he is not aware of the flow velocity although he is aware of the rate of change of velocity. Thus, for an observer moving with the particle, equations 4 become:

$$\rho_t = -\rho u_r$$

6. $$u_t = -(1/\rho)\, p_r$$

Euler ref. system, 1-dimensional inviscid, adiabatic flow referred to an observer moving with the particle.

$$e_t = -(p/\rho)\, u_r = (p/\rho^2)\, \rho_t = -\rho v_t$$

and for a three-dimensional case equation 5 gives:

$$\rho_t = -(\rho/r^2)\,(r^2 u)_r$$

7. $$u_t = -(1/\rho)\, p_r$$

Euler ref. system, 3-dimensional, inviscid, adiabatic flow referred to an observer moving with the particle.

$$e_t = -(p/r^2\rho)\,(r^2 u)_r = (p/\rho^2)\, \rho_t = -p v_t$$

As far as the Lagrangian independent variables there is no restriction on their nature as long as they are independent from each other and there are as many as the degrees of freedom. In the case of a system having one degree of freedom, the initial position can be chosen as the independent Lagrangian variable; also the mass within an initial volume is an independent variable and can be chosen as the Lagrangian coordinate. For this problem some authors used initial position and some others initial mass.

The initial position is now introduced as the independent variable. Consider an element of mass which originally is at distance (Lagrangian distance coordinate) from the origin and has a density ρ_0 and occupies the volume $\Delta \ell\, \Delta S$. Since the motion is one-dimensional at time t, ΔS has not changed but the location and the density might have changed, so that for continuity of mass

8. $$\rho_0 \Delta \ell \Delta S = \rho \Delta r \Delta S \qquad \text{Hence,} \quad \ell_r = \rho/\rho_0$$

where r is the new location.

Notice that ℓ is constant for a particle but changes from particle to particle. For a spherically symmetrical flow the element under consideration would be a thin shell, for which we can write

9. $$\rho_0 \, 4\pi \, \ell^2 \, \Delta\ell = \rho \, 4\pi \, r^2 \, \Delta r \qquad \text{Hence, } \ell_r = (\rho/\rho_0)\,(r^2/\ell^2)$$

Now the mass (L) within a certain volume, instead of the location of an initial mass (ℓ), is introduced as the Lagrangian coordinate. Let ρ_0 be the density of the matter contained between the sections r_1 and r_2 at time $t = 0$. The mass will then be:

$$L = \int_{r_1}^{r_2} k \, \rho_0 \, r^m \, dr$$

where

L = Lagrangian main coordinate

m = 0 1-Dimensional
1 Cylindrical symmetry
2 Spherical symmetry

k = ΔS 1-Dimensional
$2\pi h$ Cylindrical symmetry
4π Spherical symmetry

at any instant of time

$$L = \int_{r(r_1;t)}^{r(r_2;t)} k \, \rho \, r^m \, dr$$

making the derivative with respect to L

$$k \, \rho \, r^m \, r_L = 1$$

which, applied to a 1-dimensional case, reads:

10. $$\Delta S \, \rho \, r_L = 1 \quad \therefore \quad L_r = \Delta S \cdot \rho$$

and to a spherically symmetrical one:

11. $$4\pi \, r^2 \, \rho \, r_L = 1 \quad \therefore \quad L_r = 4\pi \, r^2 \, \rho$$

[We can compare the Lagrangian mass coordinate (L) with the Lagrangian distance coordinate (ℓ); comparing equation 8 with equation 10 (1-dimensional): $\Delta L = \rho_0 \Delta S \Delta \ell$, comparing equation 9 with equation 11 (3-dimensional spherical symmetry): $\Delta L = 4\pi \rho_0 \ell^2 \Delta \ell$, which read: the variation of the initial mass (ΔL) is equal to the initial density (ρ_0) times the variation of the initial volume ($\Delta S \Delta \ell$ or $4\pi \ell^2 \Delta \ell$), which is reasonable]. Mass momentum and energy conservation as extensively used in blast propagation problems can now be derived.

Using equations 8, equations 6 can give:

$$\ell_r = \frac{\rho}{\rho_0} \quad \text{or} \quad v_t = \frac{1}{\rho_0} u_\ell$$

12.
$$u_t = -\frac{1}{\rho} p_\ell \ell_r = -\frac{1}{\rho_0} p_\ell$$

$$e_t = -\frac{p}{\rho} u_\ell \ell_r = (p/\rho^2) \rho_t = -p v_t$$

Lagrange ref. system (position as Lagrange coord.) 1-dimensional, inviscid, adiabatic flow (Von Neumann and Richtmyer, 1950).

where the first equation for mass conservation was previously explained and the second one is:

$$\rho_t = -\rho u_r = -\rho u_\ell \ell_r = -\rho u_\ell \frac{1}{v \rho_0} = -\frac{\rho^2}{\rho_0} u_\ell$$

and therefore,

$$v_t = \frac{1}{\rho_0} u_\ell \qquad (\text{since } v = \frac{1}{\rho})$$

Using equation 9, equations 7 can give:

$$\ell_r = (r^2/\ell^2)\left(\frac{\rho}{\rho_0}\right) \quad \text{or} \quad v_t = (1/\ell^2) \frac{1}{\rho_0} (r^2 u)_\ell$$

13.
$$u_t = -\frac{1}{\rho} p_\ell \ell_r = -(r^2/\ell^2) \frac{1}{\rho_0} p_\ell$$

$$e_t = -\frac{p}{\rho} u_\ell \ell_r = (p/\rho^2) \rho_t = -p v_t$$

Lagrange ref. system (position as Lagrange coord.), 3-dimensional; inviscid, adiabatic flow with spherical symmetry (Von Neumann and Goldstine, 1955).

where the first equation for mass conservation was previously explained and the second one is:

$$\rho_t = -(\rho/r^2)\,(r^2u)_\ell\ \ell_r = -(\rho^2/\ell^2)\ \frac{1}{\rho_0}\ (r^2u)_\ell$$

and therefore

$$v_t = (1/\ell^2)\ \frac{1}{\rho_0}\ (r^2u)_\ell \qquad \left(\text{since } v = \frac{1}{\rho}\right)$$

Using equations 10, equations 6 can give:

$$L_r = \Delta S\rho \text{ or } v_t = \Delta S u_L$$

14. $$u_t = -\frac{1}{\rho}\,p_L\,L_r = -\Delta S p_L$$

$$e_t = (p/\rho^2)\,\rho_t = -p\,v_t$$

Lagrange ref. system (mass as Lagrange coord.), 1-dimensional, inviscid, adiabatic flow.

The first equation for mass conservation was previously explained and the second one is:

$$\rho_t = -\rho\,u_L\,L_r = -\Delta S\rho^2 u_L$$

and therefore

$$v_t = \Delta S u_L \qquad \left(\text{since } v = \frac{1}{\rho}\right)$$

eventually referring to a unit cross section, ΔS would be substituted by 1.

Using equations 11, equations 7 can give:

$$L_r = 4\pi r^2\rho \text{ or } v_t = 4\pi (r^2u)_L$$

15. $$u_t = -\frac{1}{\rho}\,p_L\,L_r = -4\pi r^2 p_L$$

$$e_t = (p/\rho^2)\,\rho_t = -p\,v_t$$

Lagrange ref. system (mass as Lagrange coord.), 3-dimensional, inviscid, adiabatic flow with spherical symmetry (Brode 1955-1957).

Again, the first equation for mass conservation was previously explained and the second one is:

$$\rho_t = -(\rho/r^2)\,(r^2u)_L\ L_r = -4\pi\rho^2\,(r^2u)_L$$

and therefore

$$v_t = 4\pi (r^2 u)_L \qquad \left(\text{since } v = \frac{1}{\rho}\right)$$

Eventually, referring to the mass within a steradian of the spherical shell instead of the whole shell, 4π would be substituted by 1. Equations of state and process equations will now be considered.

In this case the matter which flows is air or products of the explosion and the equation of state can be written in one of the following forms:

16a. $p\,v = f(p;T)$

16b. $p\,v = RT + bp + cp^2 + dp^3$

16c. $p\,v = RT$.

Equation 16a is very general and expresses the principle that in a gas p, v, and T are related. For a given gas the larger the range of p, v, and T, the more complicated equation 16a becomes. Often such an equation is not analytically known and experimental data must be used. For more limited ranges of p, v, and T, equation 16b provides a good approximation of equation 16a. For even more limited ranges, equation 16c can be used in place of 16a. Equation 16b and 16c are ideal simplified limits of equation 16a, just as equations 1, 2, and 3 are ideal simplified limits of more accurate expressions, particularly so if μ and k are considered constant.

Just as for the state equation, the process equation can be exact or approximated. An exact process equation is used for very few processes such as some chemical reactions. Usually one or more arbitrary restrictions on some variables of the flow take the place of the exact process equations. For instance, these restrictions may be:

17a.	$dQ = 0$	adiabatic
17b.	$ds = 0$	isentropic
17c.	$de = cdT$	polytropic (where c is any constant)
17d.	$s_t + u s_r = 0$	the flow as a whole is required to be adiabatic and reversible but the entropy is allowed to have different values at different points and to vary. It states the conservation of the entropy for the flow as a whole.

The above restrictions can be called process assumptions. The process assumptions used are at the discretion of the research worker and are justified only by the results achieved.

Moreover initial conditions and boundary conditions are also necessary to solve the problem of the blast.

The initial conditions can be:

a) A detonation wave starts at one point in the explosive, propagates through the explosive and then into air; (chemical reaction equations need to be added). The energy released is a function of the radius and the time.

b) A finite sphere of known gases surrounded by air is suddenly allowed to expand outward generating a shock wave in air and a diffusion wave in the gases (known gases here means that all the properties of the gases are known as functions of the radius; often these properties are assumed constant with the radius).

c) The overall energy is instantaneously released from an infinitesimal volume and given to the air shock.

Again condition a) is the closest to the real condition of an explosion and condition c) is the furthest.

The boundary conditions are given by the conditions in front of the shock, that is p_0, ρ_0, T_0, but Rankine-Hugoniot equations through the shock are often used, so that Rankine-Hugoniot equations act as boundary conditions. These equations specify mass, momentum,and energy conservation, for $k = \mu = 0$, one-dimensional, time independent flow, integrated with respect to the space variables. Namely they are:

$$\rho (U - u) = \rho_0 U$$

18.
$$p + \rho (U - u)^2 = p_0 + \rho_0 U^2$$

$$p/\rho + \frac{1}{2} (U - u)^2 + e = p_0/\rho_0 + \frac{1}{2} U^2 + e_0$$

which lead to the Rankine-Hugoniot equation:

19
$$\frac{1}{2} (p + p_0) \left(\frac{1}{\rho} - \frac{1}{\rho_0} \right) + \Delta e = 0$$

Applied to a perfect gas, these equations are sufficient to determine the flow properties on one side of the shock knowing those on the other side. For the pressure ratio, for instance, it is found:

$$20 \qquad \frac{p}{p_0} = \frac{(\gamma + 1)\ \rho - (\gamma - 1)\ \rho_0}{(\gamma + 1)\ \rho_0 - (\gamma - 1)\ \rho}$$

A quite complete list of similar equations is found, for instance, in NACA report 1135 (1953).

The above has defined different forms of the five necessary equations to actually compute the parameters for a blast generated shock. The solution of any of the previous sets of equations presently have to be reached numerically on digital computers. Some of the charts of the present report come from such integrations made primarily by Brode, (Reference 3); for instance Figures 15 and 16 come from Reference 3 - 1955 where the equations used were:

Conservation equations	15
Equation of State	16c
Process Assumption	17a and 17c
Boundary Conditions	18
Initial Conditions	c

An analysis of the various equations used in blast studies and of the assumptions involved is made in Reference 13. In the numerical solutions, values are found for the five dependent blast parameters: ρ, u, p, e, and T, and for some of their products like kinetic energy, static pressure impulse, and dynamic pressure impulse, as functions of the two independent blast parameters, r and t.

Blast Scaling Laws

Instead of dealing with the seven blast parameters with their dimensions, it is common practice to deal with them in dimensionless forms. This offers the advantage that any given solution can be used to calculate numerical values for several physical situations. On the other hand dimensionless solutions are often used to compute numerical values for physical situations which violate the assumptions made to non-dimensionalize the blast parameters.

It is possible to obtain a finite scaling law for shock propagation only if it is assumed that the only relevant parameter of the explosive material is its total energy. It was shown in the introduction that for several reasons that is not so for the close-field. Hence, the following considerations hold only for the far-field. They are taken essentially from Reference 14 and lead to general blast scaling laws for any atmospheric conditions.

It is assumed that the peak overpressure is a function only of R, ρ_0, c_0, and E; notice that no explosive property is considered other than its energy. Thus,

$$p = \rho\ (R;\ \rho_0;\ c_0\ ;\ E\ )$$

and applying the π - theorem of dimensional analysis, choosing mass, length, and time as fundamental dimensions, it is found that each bracketed term of the following equation is dimensionless;

$$\pi = \left(\frac{p\,R^3}{E}\right)^{a_p} \cdot \left(\frac{\rho_0\,c_0^2\,R^3}{E}\right)^{a_{\rho_0}}$$

where a_p and a_ρ are the exponents of ρ and ρ_0 respectively in the application of the π - theorem. The two terms of the π - equation are independent, since each term contains a parameter not contained in the other. The equation for p can now be written as follows:

$$\psi \left(\frac{p\,R^3}{E} \;;\; \frac{\rho_0\,c_0\,R^3}{E}\right) = 0$$

The theory of modeling is applied to the ψ - equation, after having set:

$$k_p = p^h/p^0 ;\; k_p = \rho_0^h/\rho_0 ;\; k_E = E^h/E^0 ;\; k_R = R^h/R^0 ;\; k_c = c_0^h/c_0^0$$

where superscript h and 0 indicate altitude and sea-level respectively, and subscript 0 indicate undisturbed conditions. From these, it is found that:

$$\psi\left[\frac{k_E\,p^h\,(R^h)^3}{k_p\,k_R^3\,E^h} \;;\; \frac{k_E\,\rho^h\,(c_0^h)^2\,(R^h)^3}{k_\rho\,k_c^2\,k_R^3\,E^h}\right] = 0$$

In order for the form of the solution to be the same both at sea-level and at altitude, the following relationship between the reduced altitude parameters must hold:

$$\frac{k_E}{k_p\,k_R^3} = \frac{k_E}{k_p\,k_c^2\,k_R^3} = 1 .$$

but

$$k_c^2 = \left[(\gamma\,p_0^h/\rho_0) \,/\, (\gamma\,p_0^0/\rho_0^0)\right]$$

so that from the three preceding equations k_p and k_R can be found:

$$k_p = p_0^h / p_0^0 \quad ; \quad k_R = \left[(E^h/E^0) / (p_0^h / p_0^0) \right]^{1/3}$$

and using the definitions of k_p and k_R, the following general scaling law for peak overpressure are determined:

$$p^h/p_0^h = p^0/p_0^0 \quad \text{and} \quad R^h \left[p_0^h/E^h \right]^{1/3} = R^0 \left[p_0^0/E^0 \right]^{1/3}.$$

The following general scaling law for positive impulse is also derived in Reference 14:

$$I^h \left[c_0^R/(E^h)^{\frac{1}{3}} (p_0^h)^{\frac{2}{3}} \right] = I^0 \left[c_0^0/(E^0)^{\frac{1}{3}} (p_0^0)^{\frac{2}{3}} \right]$$

When only energy is allowed to vary and atmospheric variations due to altitude are not of interest as in the case of close-to-surface explosions, the simplified scaling relationships given in Section 2.0 can be used.

To conclude this short note on scaling laws, it must be pointed out once again, that all the currently used scaling equations are based on the assumption that the energy is the only property of the explosive influencing the air blast. It was shown in the introduction that this is not true for the close-field. Thus, the results calculated or measured for a single blast of a given energy and explosive should not be used in predicting the close-field of another blast of different energy from the same explosive, much less from another explosive; particularly so if the two explosives are chemically and physically considerably different. Hence, also,the scaling laws cease to be valid for extending close-field TNT results to predict close-field propellant explosions.

APPENDIX D

GENERAL CONSIDERATIONS ON THE AIR BLAST PARAMETERS OF INTEREST IN STRUCTURAL DESIGN

Durations of Positive Phases of Overpressure and Dynamic Pressure

The uncertainty about durations of positive phases of overpressure and dynamic pressure is high because of their dependency on several factors among which are the following:

a) Nature of the explosive. The rate of energy release and the presence of secondary shocks influence the durations as shown in Figure 21.

b) Ground reflecting and absorbing properties. Very rough ground is expected to produce a thick boundary layer which alters the air flow on the surface.

c) Atmospheric temperature and pressure. The overall air blast propagation changes significantly with atmospheric conditions.

d) Ground geometrical configurations. Ground slopes produce change in the shock front and consequently in the flow which follows.

e) Wave irregularities. The actual shock wave profile is generally anything but a smooth exponential; hence, the exact zero overpressure point is more a definition than a physical entity.

f) Measuring device sensitivity. The rate of change of pressure with time when the overpressure becomes negative, is very small, hence, sensitive to any perturbance and difficult to measure exactly; the response limitations of measuring systems can give false values of actual durations (see a study of this subject in Reference 15).

Figure 22 illustrates the scatter in duration as measured and predicted. It is therefore concluded that durations for air shocks from rocket explosions have to be estimated. On the grounds of the preceding facts, the two highest curves of Figure 22 are chosen for surface blasts. These two curves are from far-field TNT measurements. Since they are considerably higher than any calculated ones, it is believed that they are already conservative and a reliability of $\pm$ 10 is estimated adequate for structural design. For inflight explosions an estimate is even more difficult because of the uncertainties previously explained to which the shock reflection - interaction problem has to be added. Hence, the rocket inflight explosion air blast durations which are presented in Figure 14 are considered reliable to $\pm$ 50 percent.

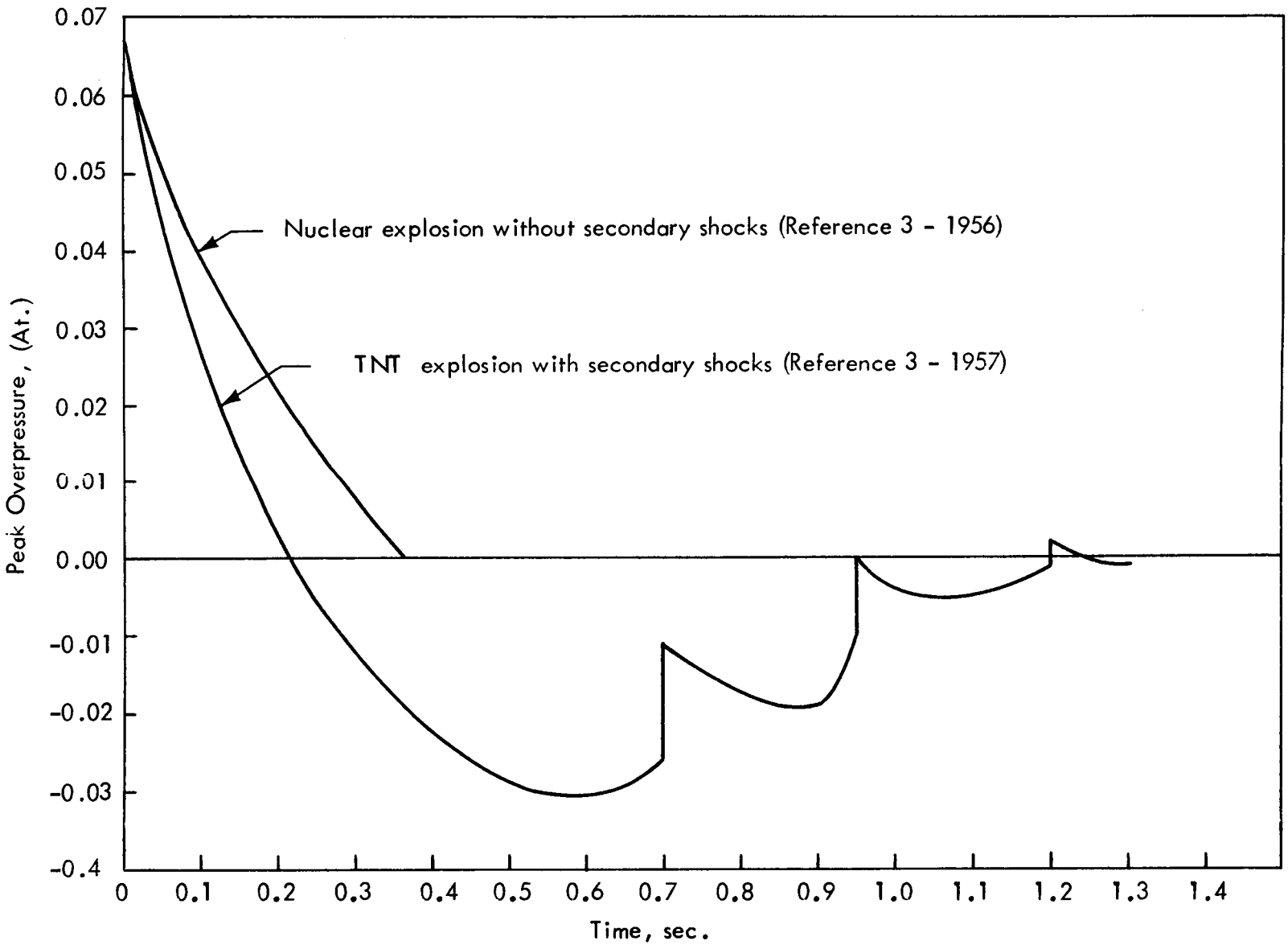

Figure 21: Theoretical Overpressure Time Histories at a Distance of 4,400 feet for Two 10^6 lb Far-Field-TNT-Equivalent Surface Explosions

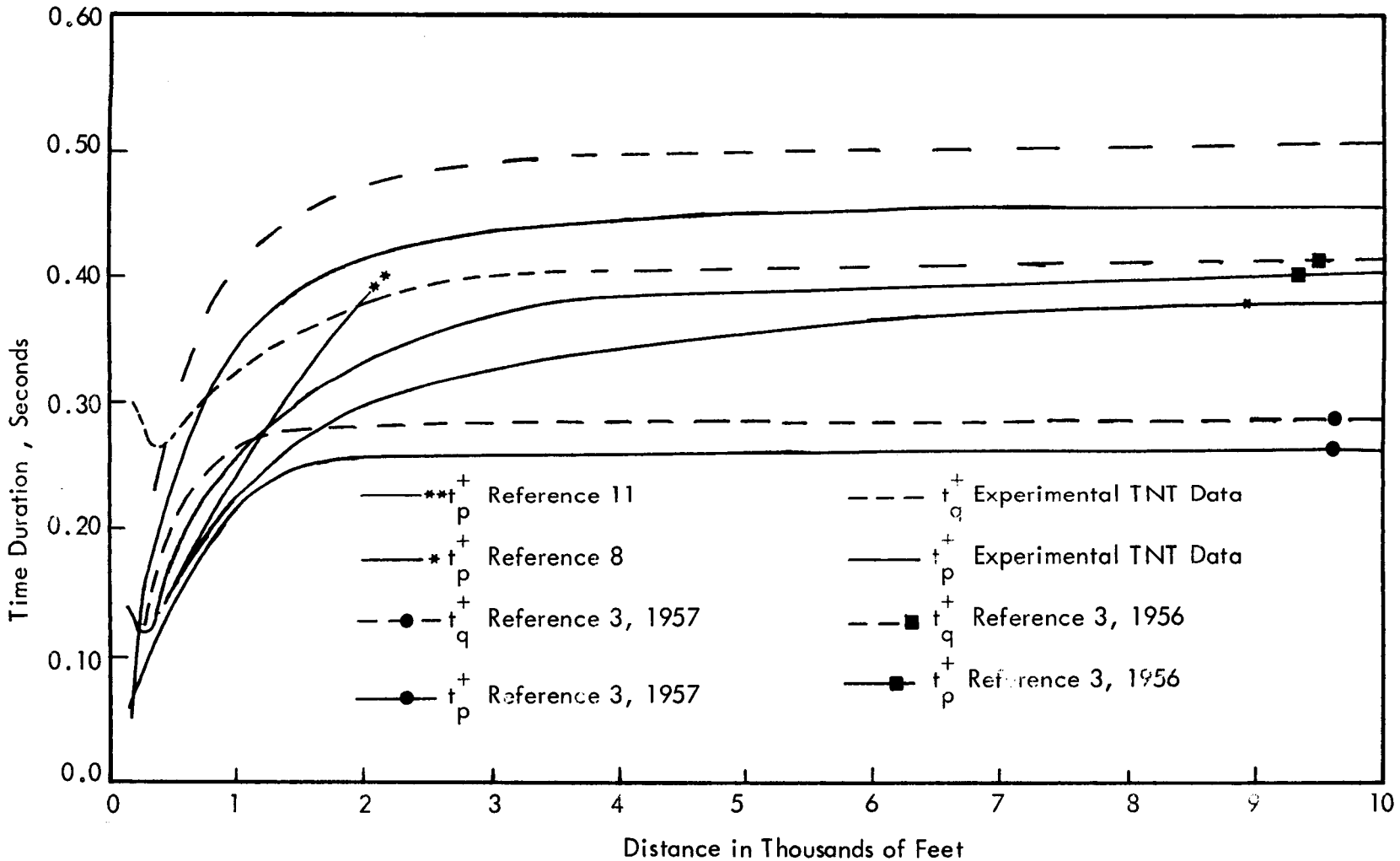

Figure 22: Duration of Positive Phases of Overpressure and Dynamic Pressure for a 10^6 lb Far-Field-TNT-Equivalent Surface Explosion

Time Variations of Overpressure and Dynamic Pressure

The best way to calculate the time variation of overpressure and dynamic pressure at any given distance from ground zero of a rocket explosion would be to make a numerical integration of the pertinent blast equations with the proper initial conditions and the proper time rate of energy release. This point has already been sufficiently stressed throughout the present report. However, for far-field-TNT-equivalencies of the order of 5×10^6 lbs. and peak overpressures less than 14.7 psi, time variations of overpressure and dynamic pressure of the air shock from a rocket explosion can be estimated rather accurately from TNT and nuclear explosion studies provided that peak overpressure, peak dynamic pressure, and time durations of positive overpressure and dynamic pressure, in turn have been estimated accurately.

From experimental results for large explosion, (Reference 16 for instance), it is found that for overpressures less than 14.7 psi, or dynamic pressures less than 4.7 psi, the overpressure decays almost linearly with time while the dynamic pressure, already small, also exponentially approaches zero so that its influence tends to be negligible. Hence, for peak overpressure less than 1.47 psi, a linear variation for the pressure has been assumed and the dynamic pressure neglected. For peak overpressures greater than 1.47 but less than 14.7 psi, Brode's calculations for a point source of energy release have been used even though there are available calculations for TNT explosions. The reason for such a choice is that TNT calculations consider secondary shocks which are not considered in the point source section. For liquid propellants explosion, secondary shocks would be very weak, thus, the main shock would be more like the shock from a point source than from a TNT charge. Naturally, the above reasoning holds only for the far-field.

Peak Dynamic Pressure Versus Peak Overpressure and Dynamic Pressure Sensitive Structures

Obstacles with closed cross sectional area of the order of 1.0 $ft.^2$ or less are ordinarily affected more by the dynamic pressure than by the overpressure. The reason being that it usually takes only a small fraction of the natural period of oscillation of the obstacle for the shock front to travel from the front area of the obstacle to the back face of it. Thus, the static pressure becomes almost equal on every face of the obstacle before the latter has the time to react to the initial static pressure load. On the other hand, the wind which follows the shock lasts long enough for the obstacle to react to it. The force per unit area on wind-sensitive obstacles (power lines, antennas, and wires, etc.), is the product of the dynamic pressure and appropriate drag coefficients. The dynamic pressure for a peak overpressure greater than 1.47 psi was given in Section 4.0. Dynamic pressure for a peak overpressure less than 1.47 psi will be neglected on the grounds of the following arguments:

a) Figure 23 shows that for a normal shock with a peak overpressure less than 1.47 psi the peak dynamic pressure is less than 1/27 of the peak overpressure.

b) A dynamic pressure of 1.47/27 psi = 7.8 psf, corresponding to a steady wind velocity of 56 miles per hour, (see Figure 24), is acceptable for wind sensitive obstacles since it is less than the minimum design wind pressures shown in Figure 25, even when allowance is made for dynamic magnification of response to the transient blast wind. The design

wind pressures in Figure 25 have been established by the American Standards Association in References 17 and 18, and are based on the fastest-single-mile wind speed (see Reference 18) multiplied by a gust factor dependent on height (1.3 at 30 ft.). The corresponding dynamic pressure is then multiplied by a shape factor of 1.3 to define the net lateral wind pressure.

c) Figures 15 and 16 show that the dynamic pressure decays faster than the static pressure (or overpressure) even if it has a longer positive phase duration as shown by Figure 13.

d) The drag coefficient or shape factor can vary from - 0.5 to + 2.0, thus leaving substantially valid the above arguments.

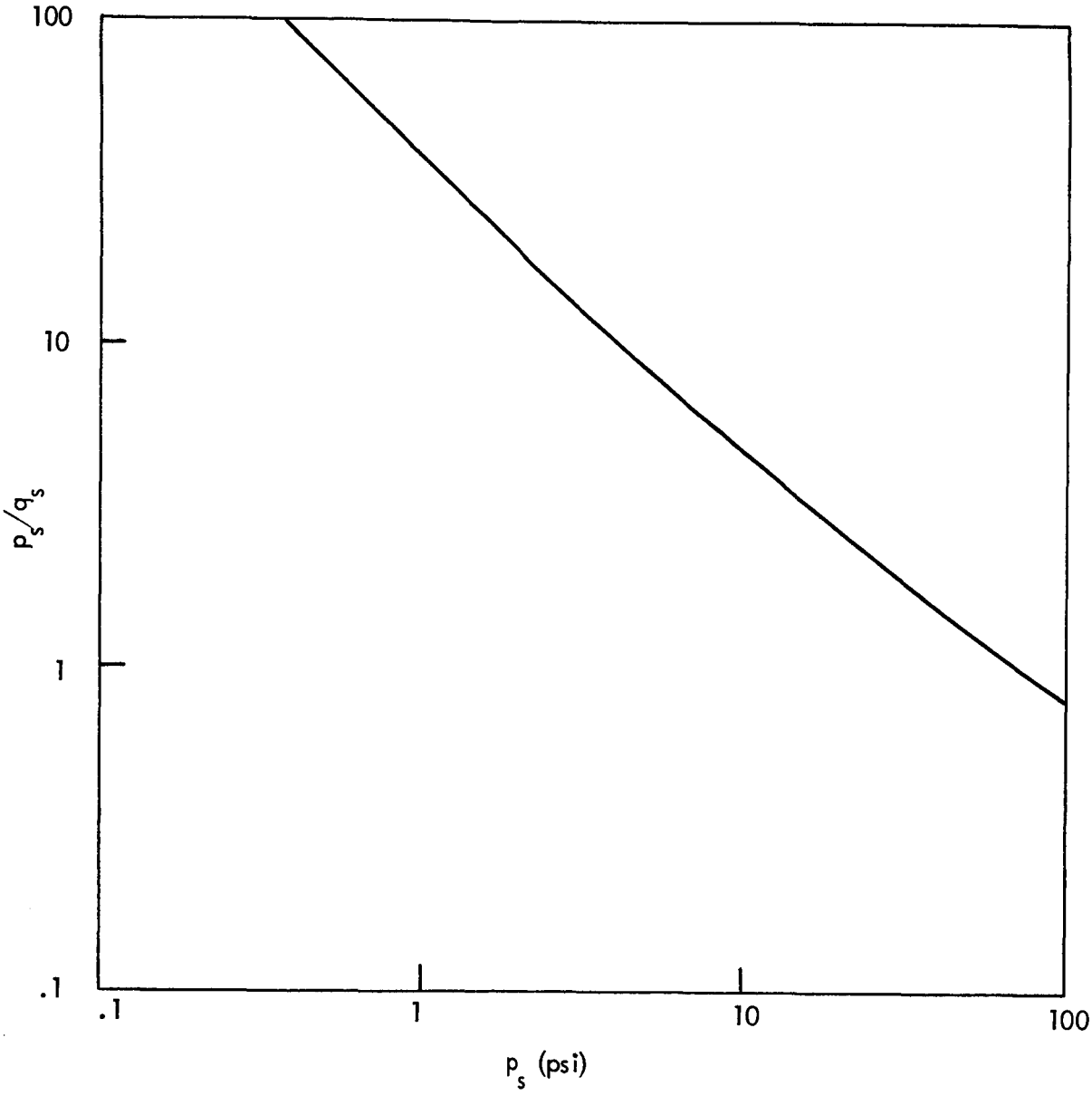

Figure 23. Ratio of Peak Overpressure to Peak Dynamic Pressure versus Peak Overpressure for a Normal Shock

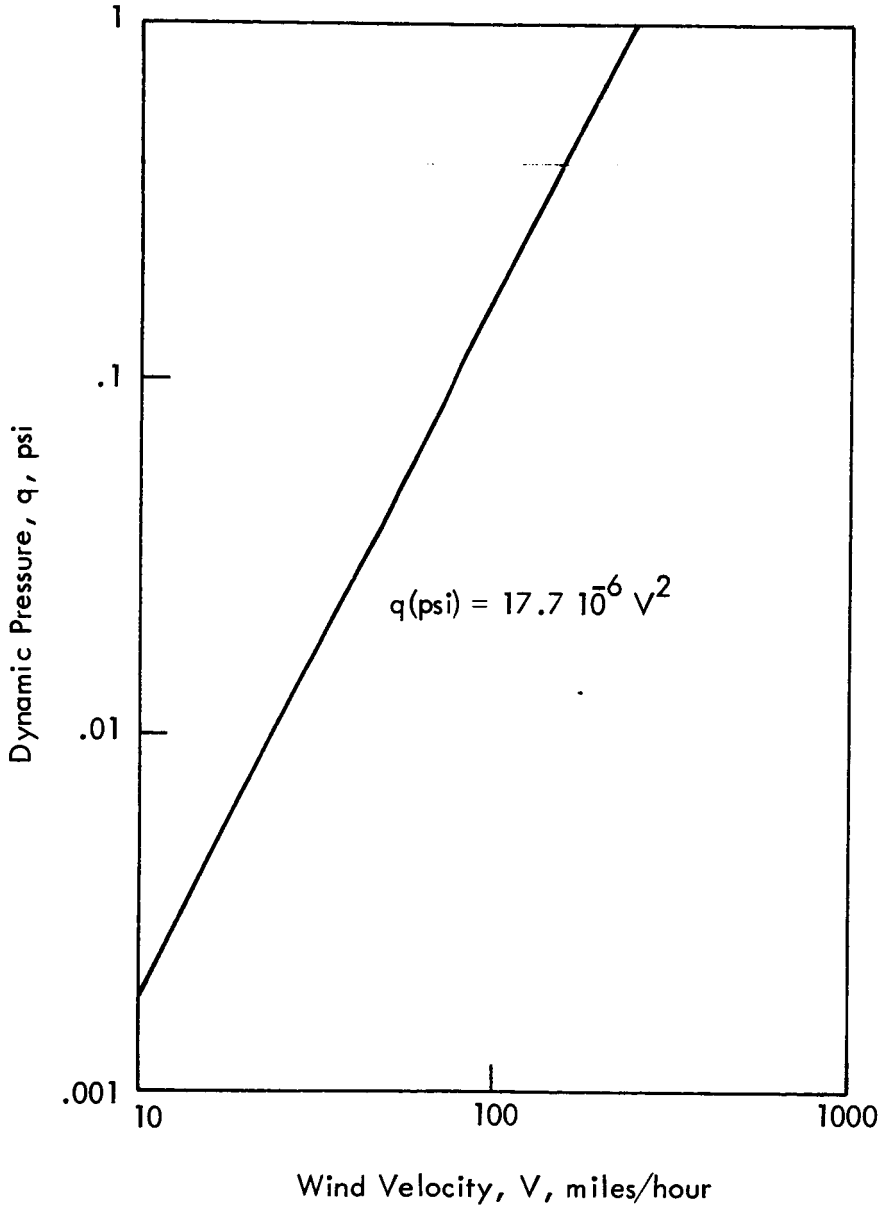

Figure 24. Dynamic Pressure versus Wind Velocity

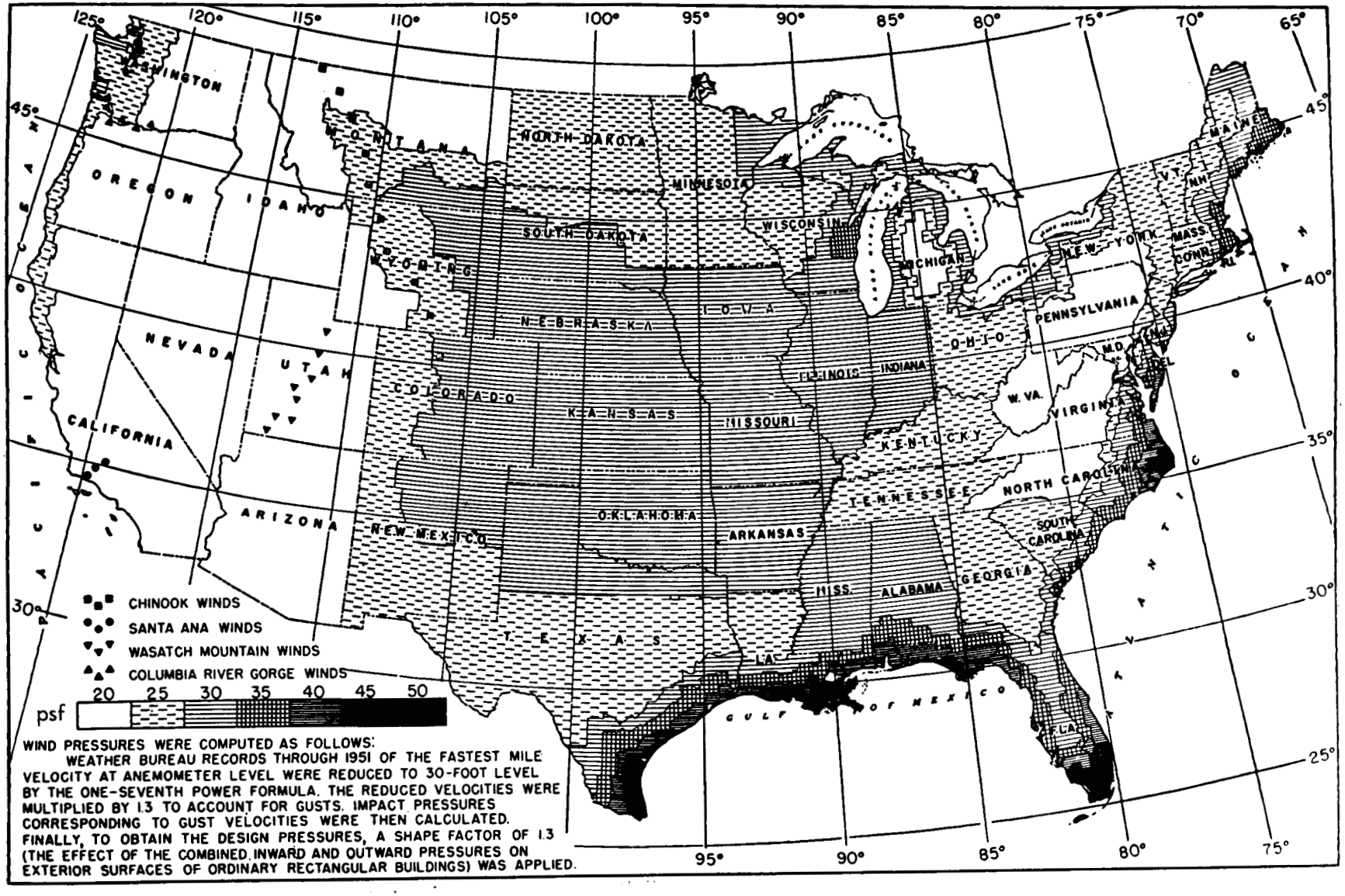

Figure 25: U. S. Wind Pressure Map

From: Building Construction Handbook, F. S. Merritt Editor, Copyright © (1958), McGraw Hill.
Used by Permission of McGraw Hill Book Company

APPENDIX E

TABLE V

STRUCTURAL DAMAGE CRITERIA FOR BLAST ENERGY OF THE ORDER OF 10 KILOTONS

The following table is self-explanatory. A more complete analysis of blast loads on structures will be covered in a subsequent report.

Approximate Side on Peak Overpressure Ranges (psi)	Obstacle Definition and Damage Ranges
$p_s \leq .02$	No damage expected.
.02 - .5	Window Damage.
.5 - 1.0	Usual shattering of large and small glass windows; occasional frame failure. Light damage to aircrafts (flight possible, performances restricted).
1.0 - 2.0	Shattering of corrugated asbestos siding, failure of connection of corrugated steel of aluminum paneling followed by buckling. Moderate damage to aircraft (field maintenance required to restore aircraft to operation status). Light forest damage (equivalent wind up to 80 miles per hour).
2.0 - 3.0	Moderate damage to wood-frame building and residential type; shattering of concrete or cinder-block 8 or 12 inch thick wall panels. Severe damage to aircrafts. Forest damage: up to 30 percent of trees blown down (equivalent wind up to 110 miles per hour).
3.0 - 4.0	Severe damage to wood frame residential type building and moderate damage to wall-bearing masonry building (apartment-house type). Forest damage: up to 80 percent of trees blown down (equivalent wind up to 125 miles per hour).

5.0 - 6.0	Severe damage to wall-bearing masonry building (apartment-house type).
6.0 - 7.0	Moderate damage to multi-story wall-bearing building, (monumental type).
7.0 - 11.0	Severe damage to multi-story wall-bearing building, (monumental type). Shearing and flexure failures of brick wall panel - 8 to 12 inches thick. Moderate damage to reinforced concrete (not earthquake-resistent) buildings and concrete walls.
11.0 - 15.0	Severe damage to reinforced concrete (not earthquake-resistent) building and concrete walls.
30.0 - 40.0	Damage to ventilation and entrance door of shallow buried structures [light, corrugated steel arch, surface structure (10 gage corrugated steel with a span of 20 to 25 feet) Central angle of 180° with 5 feet of earth cover at the crown] .
40.0 - 50.0	Moderate damage to the immediately above described structures (large deformations of end walls and arch and major entrance doors).
45.0 - 60.0	Collapse of the above described structures.
120.0 - 160.0	Light damage (cracking of panels, possible entrance door damage) to buried concrete arch with a 16 foot span and central angle of 180°; 8 inch thick with 4 feet of earth cover at the crown.
160.0 - 220.0	Moderate damage (large deformations with considerable cracking and spalling) to the above described structures.
220.0 - 280.0	Collapse of the above described structures.

Whenever not specified, light, moderate, and severe damages have the following meaning:

Light Damage:	The object can still perform its functions, small repairs will suffice.
Moderate Damage:	The object cannot perform its functions any more but repair is still possible and economically feasible.
Severe Damage:	The object has collapsed or has been damaged beyond repair.

It is important to notice that for a given peak overpressure there is only one peak dynamic pressure but the durations of the positive phases increase with the total energy of the explosion. The above table comes primarily from tests with atomic explosions on the order of 20 kilotons. A 20 kiloton atomic explosion is equivalent to a 10 kiloton actual TNT charge as far as the air blast is concerned, because only 50 percent of the atomic energy is released as air shock. In Section 3.0, it was seen that the largest of the future liquid propellant rockets may be expected to have a maximum far-field-TNT-equivalent of about 5×10^6 lbs. = 2.5 kiloton. Hence, the above table can be considered somewhat conservative as far as rocket explosions are concerned, because for the same peak overpressure, the duration of the positive phases will be shorter. This is particularly so for drag sensitive structures like power lines, trees, and poles.

According to the preceding table, the following conclusions can be reached for ranges of structural damage:

a) For peak overpressure $\leq .02$, no damage.

b) Outside the radius at which the blast side-on overpressure is greater than .02 psi, but less than 1 psi, conventional houses and life support facilities would suffer minor damage. Human life would not be endangered although injuries might occur.

c) Within the radius in which the blast side-on overpressure is greater than 1 psi, but less than 10 psi, conventional houses and life support facilities would suffer serious damage and man would suffer severe injuries and occasional fatalities. Nevertheless, relatively minor modifications to conventional structures would enable them to resist serious damage and to protect man.

d) Within the radius where the side-on peak overpressure is greater than 10 psi, only blast designed structures would resist damage and be able to protect human life.

Blast injuries to man are of two main types: direct, from overpressure and indirect from body displacement or from missile-like broken glass.

Criteria for these two types of blast injuries are summarized in the following table. They are taken from Reference 19.

Direct

		Peak Incident Pressure	
		Without Reflection	With Reflection
Eardrum Rupture	- Threshold	5 psi	2.3 psi
Lung Hemorrhage	- Threshold	15 psi	6.4 psi
Fatal Internal Injuries	- 1 Percent Lethality	30-42 psi	12-15 psi

Indirect

		Related Velocity
Cerebral Concussion by 10 lb. Missile	- Threshold	10 ft/sec.
Skull Fracture, by 10 lb. Missile	- Threshold	10 ft/sec.
Serious Wound by 10 g glass Fragment	- Threshold	100 ft/sec.
Skin Lacerations by 10 g glass Fragment	- Threshold	50 ft/sec.

It has been found in Reference 11 that there is only a one percent probability of glass fragments penetrating the abdominal cavity (equivalent to a serious wound by glass noted above) of a peak side-on overpressure of 3 psi. It is estimated, therefore, that the threshold for skin lacerations from glass fragments would be at overpressures of about 1.5 psi.

REFERENCES

1. Taylor, G.: The Formation of a Blast Wave by a Very Intense Explosion; Proc. Roy. Soc. London A 201 (159 - 186) Written in 1941, Published in 1950. Other works by Taylor, G. on related subjects:
   Proc. Roy. Soc. A, 84, 371 1910
   Proc. Roy Soc. A, 186, 273 1946
   Proc. Roy Soc. A 200, 235 1950
   Proc. Roy Soc. A, 219, 186 1953
   Proc. Roy Soc. A, 225, 473 1954

2. Bethe, H. A.; Fuchs, K.; Hirsc Felder, J. G.; Magee, J. L.; Peierls, R. E.; and Von Neuman, J.: Blast Wave; Los Alamos Report 2000, 1947.

3. Brode, H. L.: Numerical Solution of Spherical Blast Waves; J. App. Physics, Vol. 26, (786), 1955.
   Point Source Explosions in Air; The Rand Corp., Research Memo RM-1824-AEC, 1956.
   The Blast Wave in Air Resulting From A High Temperature High Pressure Sphere of Air; The Rand Corp., Research Memo RM-1825-AEC, 1956.
   A Calculation of the Blast Wave From A Spherical Charge of TNT AD 144302, 1957
   Blast Wave From A Spherical Charge; The Physics of Fluids, Vol. 2, No. 2, March-April, 1959.
   A Review of Nuclear Explosion Phenomena Pertinent to Protective Construction; R-425-PR, 1964.

4. D.O.D. Document 4145-21: Quantity-Distance Storage Criteria for Liquid Propellants; 21-March, 1964.

5. Cook, M. A. and Udy, L. L.: Detonation Pressure of Liquid Hydrogen/Liquid Oxigen; Intermountain Research and Engineering Co.; Final Report on Contract No. NAS 8-5058, 1962.

6. Oslake, J. J.; et al: Explosive Hazard of Rocket Launchings; Aeronutronics, Technical Report No. U-108, 98, 1960.

7. Baum, F. A.; Stanyukovich, K. P.; and Shekhter, B. I.: Physics of an Explosion; AD 400151, Russian book, Fizmatoiz, Moscow, 1959.

8. Holmes and Narver, Inc. Ed.: Design Manual AEC Test Structures, TID-16347, 1961.

9. Rudlin, L.: On the Origin of Shock Waves From Spherical Condensed Explosions in Air; Part I, AD 4 14 637, 1963.

10. Sommers; and Morrison: Simulation of Condensed-Explosive Detonation Phenomena With Gases; The Physics of Fluid, Vol. 5, No. 2, (241-248), 1962.

11. Glasstone, S.; (ed): The Effects of Nuclear Weapons; U. S. Dept. of Defense, U. S. Atomic Energy Comm., 1962.

12. Pack, D. C.: The Reflection and Transmission of Shocks; Part I, The Reflection of A detonation Wave at a Boundary; Phil Mag. 2, 182, 1957.

13. Bracco, F. V.: A Method for Predicting the Air Blast Parameters From Liquid Propellant Rocket Explosions; Wyle Laboratories Report WR-64-11, 1964.

14. Sperrazza, J.: Modeling of Air Blast; Amer. Soc. of Mech. Engrs. Proceedings of the Winter Annual Meeting (65 - 70), 1963.

15. Crocker, M. J.; and Sutherland, L. C.: The Effects Upon Shock Measurements of Limited Frequency Response Instrumentation; Wyle Laboratories Report WR- 65-1, 1965.

16. Kincery, C. N.; Keefer, J. H.; and Day, J. D.: Surface Air Blast Measurements From A 100-Ton TNT Detonation; B.R.L. Memorandum Report No. 1410, 1962.

17. American Standard Building Code Requirements for Minimum Design Loads in Buildings and Other Structures, A 58.1, (Revision 1955). Note: A bibliography on the problem of the air blast from explosions is found in Reference 13.

18. Brekke, G. N.: Wind Pressures in Various Areas of the United States; National Bureau of Standards, Building Materials and Structures Report 152, April 24, 1959.

19. White, C. S.: Tentative Biological Criteria for Assessive Potential Hazards From Nuclear Explosions; Lovelace Foundation for Medical Education and Research, Albuquerque, N. M., DASA 1462, 1963.